A Short Review of Classical & Quantum Active Matter

Leticia F. Cugliandolo

Sorbonne Université

leticia@lpthe.jussieu.fr

www.lpthe.jussieu.fr/~leticia

XXVIII Giambiagi School, Buenos Aires, 2026

Plan

1. Classical Active Matter
   - Real and artificial systems
   - Models
   - Phenomenology
2. Quantum Active Matter
   - Models
   - Phenomenology
   - Realizations ?
3. Perspectives

Plan

1. **Classical Active Matter**
   - Real and artificial systems
   - Models
   - Phenomenology
2. Quantum Active Matter
   - Models
   - Phenomenology
   - Realizations ?
3. Perspectives

Interacting Many-Body Systems

Some examples

Many-body systems

Some examples

Ferromagnetic Ising Model

$$\mathcal{V} = -\frac{J}{2} \sum_{\langle ij \rangle} s_i s_j$$

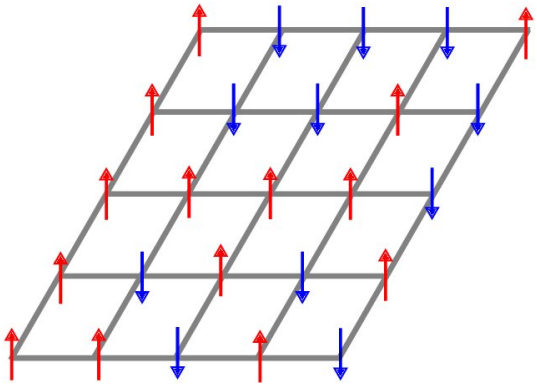

Particles in Interaction

$$\mathcal{V} = \sum_{i \neq j} V(r_{ij})$$

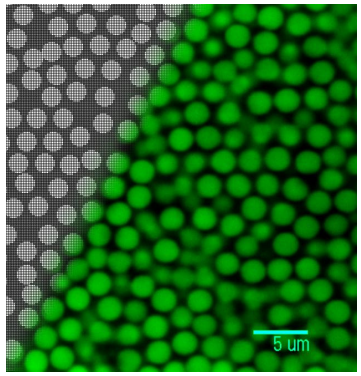

Active Matter

$$\boldsymbol{F}_i \neq -\boldsymbol{\nabla}_i \mathcal{V}$$

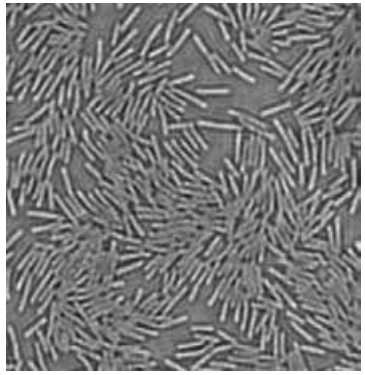

In physical systems the action-reaction principle is respected, in other examples it is not

Many examples beyond physics, like **ecosystems, markets**, etc. $\boldsymbol{F}_{i \to j} \neq \boldsymbol{F}_{j \to i}$

non-reciprocal interactions

Active Matter

Definitions and realisations

Active Matter

Definition - Biological inspiration

Active matter is composed of large numbers of active "agents", which consume energy and thus move or exert mechanical forces

Due to the energy consumption, these systems are intrinsically out of thermal equilibrium

Homogeneous energy injection (not from the borders, *cfr.* shear)

Coupling to the environment (bath) allows for dissipation

Active Matter

Natural & artificial systems

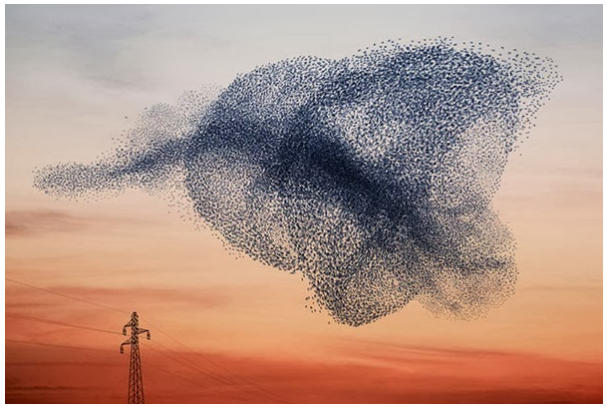

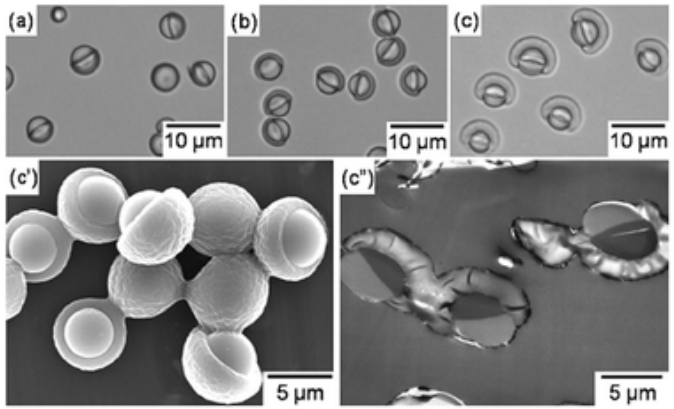

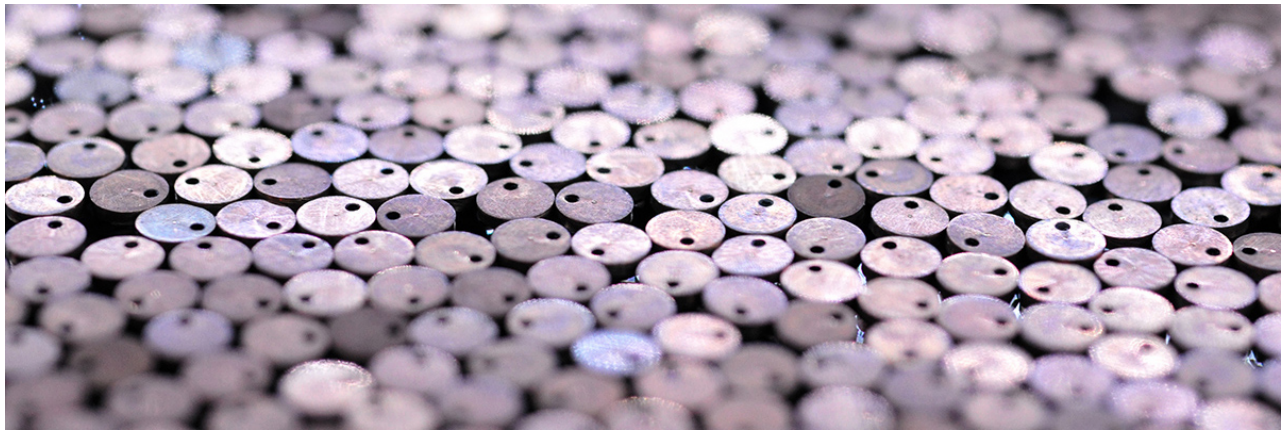

Experiments & observations **Bartolo et al.** Lyon, **Bocquet et al.** Paris, **Cavagna et al.** Roma, **di Leonardo et al.** Roma, **Dauchot et al.** Paris, just to mention some Europeans

Active matter

Realisations & modelling

- Wide range of scales: macroscopic to microscopic

  Natural examples are birds, fish, cells, bacteria.

  Artificial realisations are Janus particles, asymmetric grains, toys, etc.

- Embedding spaces in $3d$, $2d$ and $1d$.
- Particle shapes

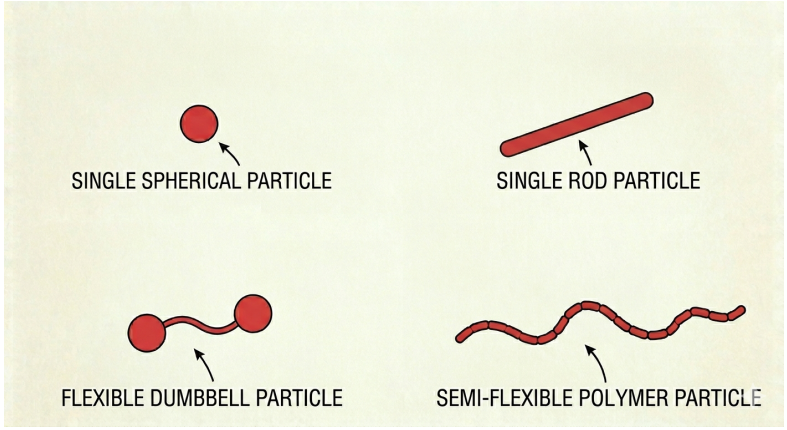

- Self-propulsion mechanism

  Microscopic - details often ignored

- Energy injection mechanism

  Details ignored - models proposed

  Non-conservative forces

Active Matter

Global goal - from our "community"

To understand the **collective** behaviour of **active matter**

from the **statistical physics** viewpoint

with the help of extensive **numerical simulations**

and **theoretical arguments/analytic calculations**

Statistical Physics approach

One has to start from the **single particle/hydro/field theory** modelling

Single Spherical Particle Models

Brownian Motion

Langevin description

A spherical particle immersed in a liquid

Force on the particle due to the collisions with the liquid molecules

No external force

$$\overbrace{m\ddot{\boldsymbol{r}} = \boldsymbol{F}_{\text{env}}}^{\text{Newton}} = \underbrace{-\gamma\dot{\boldsymbol{r}}}_{\text{friction}} + \underbrace{\boldsymbol{\xi}}_{\text{noise}}$$

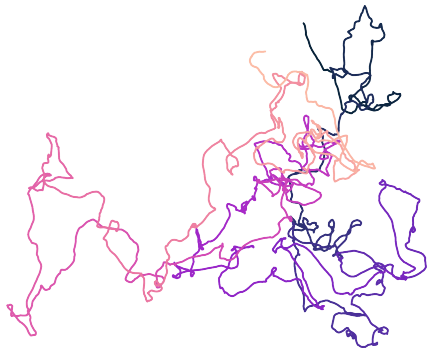

$\boldsymbol{\xi}$ Gaussian white noise with $\langle \xi_a(t) \rangle = 0$ and $\langle \xi_a(t)\xi_b(t') \rangle = 2\gamma k_B T \delta_{ab}\delta(t-t')$

$a, b = 1, \ldots, d$

Averaged position $\langle \boldsymbol{r}(t) \rangle = \boldsymbol{r}_0$ the initial position

Einstein 05, Smoluchowski 06, Langevin 08, Fokker-Planck 14-17

Brownian Motion

Proof of molecular nature of matter

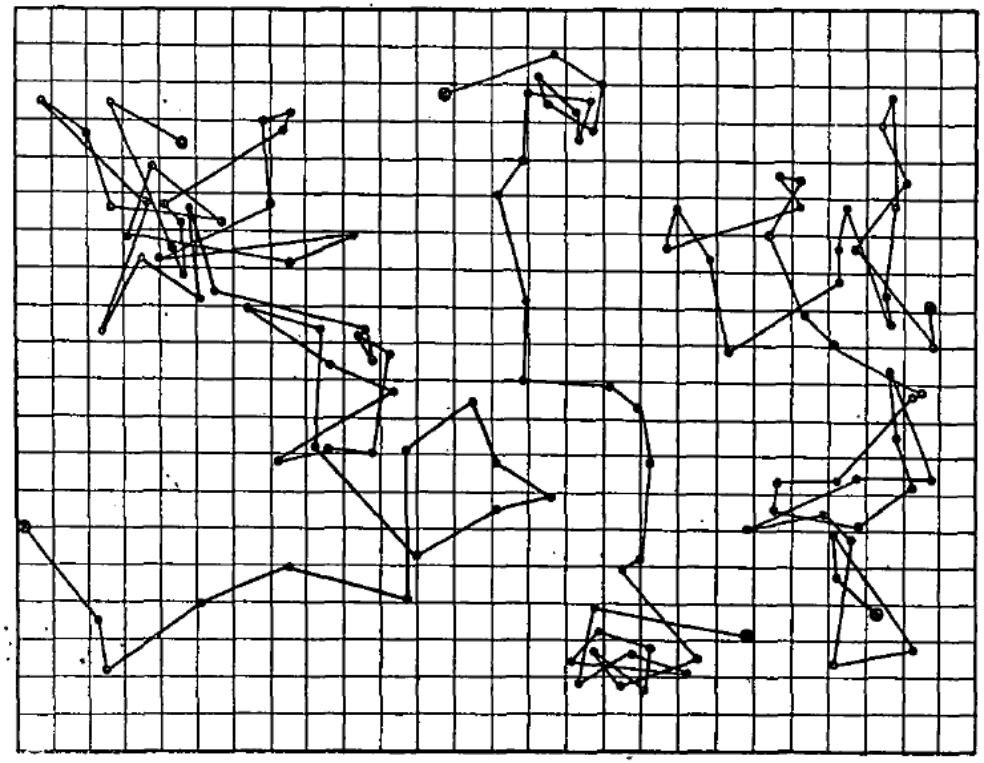

Trajectories of three tracers embedded in a shallow molecular liquid

Perrin 09 *"Brownian motion and molecular reality"*

Brownian Motion

Langevin description

A spherical particle immersed in a liquid

Force on the particle due to the coupling to the environment

No external force

$$\overbrace{m\ddot{\boldsymbol{r}} = \boldsymbol{F}_{\text{env}}}^{\text{Newton}} = \underbrace{-\gamma\dot{\boldsymbol{r}}}_{\text{friction}} + \underbrace{\boldsymbol{\xi}}_{\text{noise}}$$

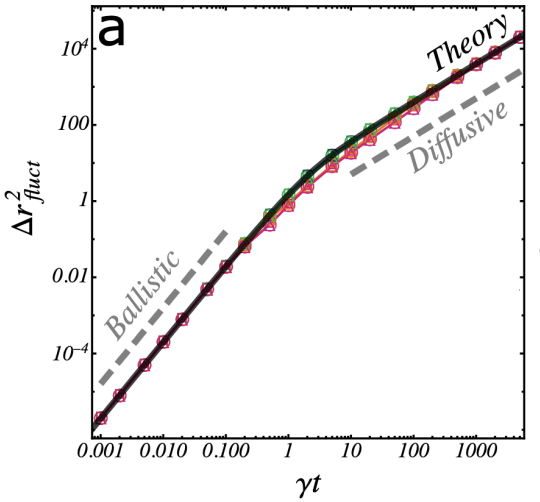

Mean-square displacement $\Delta^2(t,0) = \langle(\boldsymbol{r}(t) - \boldsymbol{r}_0)^2\rangle$

At $t < {}^{m}/_{\gamma}$ *ballistic* $\Delta^2 \propto t^2$

At $t > {}^{m}/_{\gamma}$ *diffusive* $\Delta^2 \propto D_T\, t$

Diffusion coefficient $D_T = {}^{k_B T}/_{\gamma}$

Active Brownian Sphere

Langevin equations

Active force $f_{\rm act}$ along $\hat{\boldsymbol{n}} = (\cos\theta, \sin\theta)$ a direction following a random walk

$$\begin{aligned} m\ddot{\boldsymbol{r}} &= f_{\rm act}\hat{\boldsymbol{n}} - \gamma\dot{\boldsymbol{r}} + \boldsymbol{\xi} \\ \dot{\theta} &= \eta \end{aligned}$$

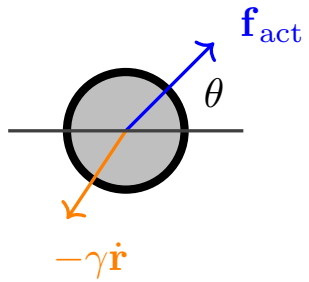

$\boldsymbol{\xi}$ and η Gaussian white noises

$\langle \xi_a(t)\rangle = \langle \eta(t)\rangle = 0$, $\langle \xi_a(t)\,\xi_b(t')\rangle = 2\gamma k_B T\delta_{ab}\delta(t-t')$ and $\langle \eta(t)\,\eta(t')\rangle = 2D_\theta\delta(t-t')$

Persistence time $\tau_p = 1/D_\theta$ and length $\ell_p = v_0\,\tau_p = (f_{\rm act}/\gamma)\,\tau_p$

Péclet number Pe = $f_{\rm act}\sigma/(k_BT)$ measures the activity

Active Brownian Sphere

Langevin equations

Active force $f_{\rm act}$ along $\hat{\boldsymbol{n}} = (\cos\theta, \sin\theta)$ a direction following a random walk

$$
\begin{aligned}
m\ddot{\boldsymbol{r}} &= f_{\rm act}\hat{\boldsymbol{n}} - \gamma\dot{\boldsymbol{r}} + \boldsymbol{\xi} \\
\dot{\theta} &= \eta
\end{aligned}
$$

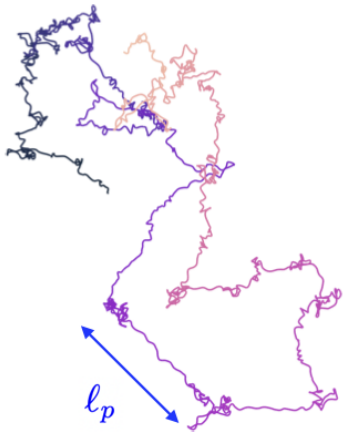

$\boldsymbol{\xi}$ and η Gaussian white noises

$\langle \xi_a(t) \rangle = \langle \eta(t) \rangle = 0$, $\langle \xi_a(t)\, \xi_b(t') \rangle = 2\gamma k_B T \delta_{ab} \delta(t-t')$ and $\langle \eta(t)\, \eta(t') \rangle = 2D_\theta \delta(t-t')$

Persistence time $\tau_p = 1/D_\theta$ and length $\ell_p = v_0\, \tau_p = (f_{\rm act}/\gamma)\, \tau_p$

Péclet number Pe = $f_{\rm act}\sigma/(k_B T)$ measures the activity

Active Ornstein Uhlenbeck

Over-damped Langevin equations

Long times, beyond the inertia time-scale $t \gg {}^{m}/_{\gamma}$

$$\dot{\boldsymbol{r}} = \boldsymbol{v} \qquad\qquad \tau\,\dot{\boldsymbol{v}} = -\boldsymbol{v} + \boldsymbol{\eta}$$

Gaussian white noise with $\langle \eta_a(t) \rangle = 0$ and $\langle \eta_a(t)\eta_b(t') \rangle = 2D\,\delta_{ab}\,\delta(t-t')$

The random velocity $\boldsymbol{v}$ is correlated as

$$\langle v_a(t) v_b(t') \rangle = \delta_{ab}\,\frac{D}{\tau}\,e^{-|t-t'|/\tau}$$

Unbalanced correlated noise and memoryless friction $\Longrightarrow$

out-of-equilibrium environment

Similar **phenomenology** as the one of the ABPs but simpler to deal with,

no additional degree of freedom **Martin et al 21**

ABP & AOUP

Mean-square displacement

$$\Delta^2(t) \equiv \langle (\boldsymbol{r}(t) - \boldsymbol{r}(0))^2 \rangle = \langle (\boldsymbol{r}(t) - \boldsymbol{r}_0)^2 \rangle = \langle (\boldsymbol{r}(t) - \langle \boldsymbol{r}(t) \rangle)^2 \rangle \equiv \mathrm{Var}(\boldsymbol{r}(t))$$

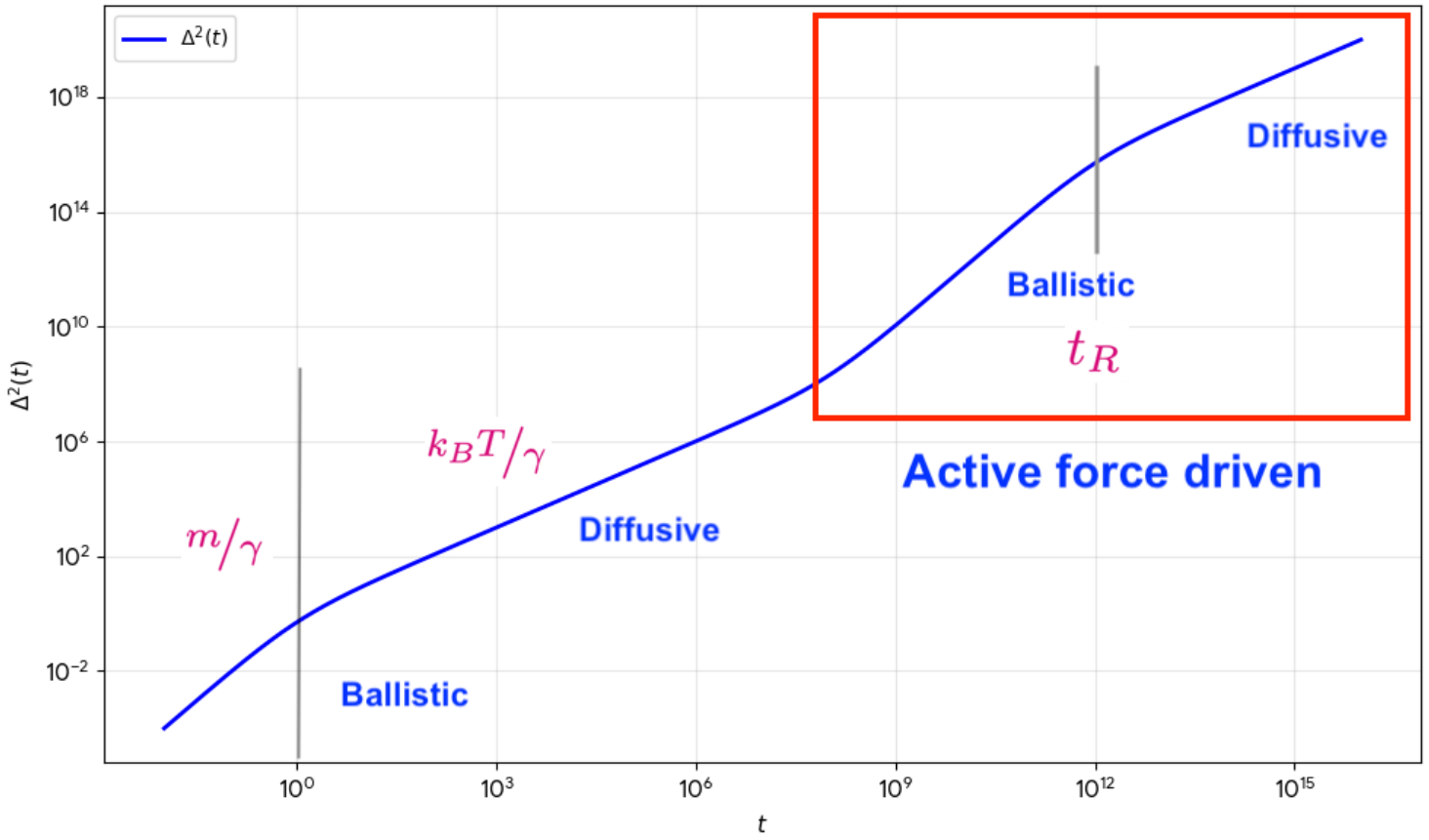

Active Brownian Sphere

Mean-square displacement

Active force f_{act} along $\hat{\boldsymbol{n}} = (\cos\theta, \sin\theta)$ a direction following a random walk

$$m\ddot{\boldsymbol{r}} = f_{\mathrm{act}}\hat{\boldsymbol{n}} - \gamma\dot{\boldsymbol{r}} + \boldsymbol{\xi} \qquad \dot{\theta} = \eta$$

Mean-square displacement $\Delta^2(t) = \langle(\boldsymbol{r}(t) - \boldsymbol{r}(0))^2\rangle$

Time	Regime	$\Delta^2 \propto$	Physical Interpretation
$t < {}^{m}/_{\gamma}$	ballistic	${}^{k_BT}/_{m}\, t^2$	Inertial thermal velocity dominates
${}^{m}/_{\gamma} < t < \tau^*$	diffusive	$D_T\, t$	Damping $\mapsto$ thermal Brownian motion
$\tau^* < t < t_R$	ballistic	${}^{f_{\mathrm{act}}^2}/_{\gamma^2}\, t^2$	Self-prop speed $v_0 = {}^{f_{\mathrm{act}}}/_{\gamma}$ dominates
$t_R < t$	diffusive	$D_A\, t$	Rotational diffusion randomizes $\boldsymbol{v}_0$

Diffusion coefficients $\underbrace{D_T = {}^{k_BT}/_{\gamma}}_{\textbf{thermal}} \qquad \underbrace{D_A = D_T + c\,\mathrm{Pe}^2}_{\textbf{active}}$

Active Brownian Particles

Aggregation close to walls

Active force $f_{\rm act}$ along $\hat{\boldsymbol{n}} = (\cos\theta, \sin\theta)$ a direction following a random walk

$$m\ddot{\boldsymbol{r}} = f_{\rm act}\hat{\boldsymbol{n}} - \gamma\dot{\boldsymbol{r}} + \boldsymbol{\xi} \qquad \dot{\theta} = \eta$$

Motion of Janus colloids & ABPs

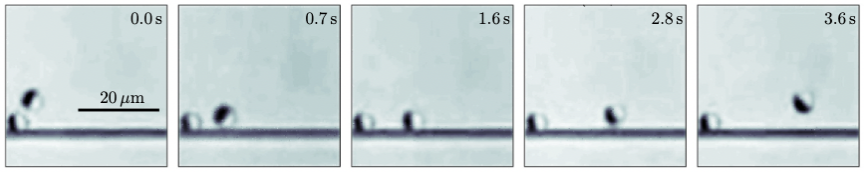

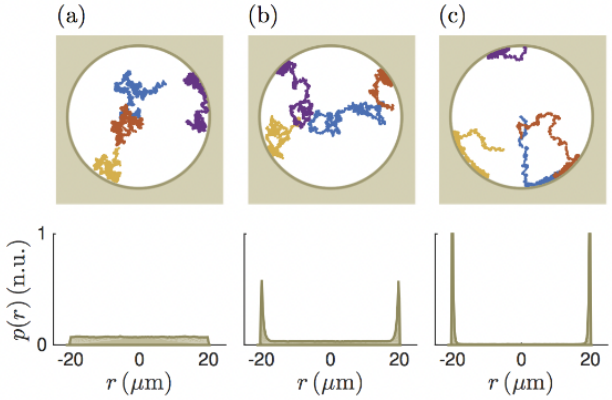

close to a wall **in a pore**

Many-Body Models

Vicsek model

Minimal (cellular automata) model for flocking

Flocking due to any kind of self-propulsion and alignment with neighbours

The individual's direction is updated according to the mean $\overline{\ldots}$ over its neighbours

$$\hat{\boldsymbol{v}}_i(t+\delta t) = \overline{\hat{\boldsymbol{v}}_j(t)}_{|\boldsymbol{r}_i-\boldsymbol{r}_j|<r_0} + \boldsymbol{\eta}_i(t)$$

plus noise & normalization

moves at constant speed v_0 in the new direction

$$\boldsymbol{r}_i(t+\delta t) = \boldsymbol{r}_i(t) + v_0\hat{\boldsymbol{v}}_i(t+\delta t)\,\delta t$$

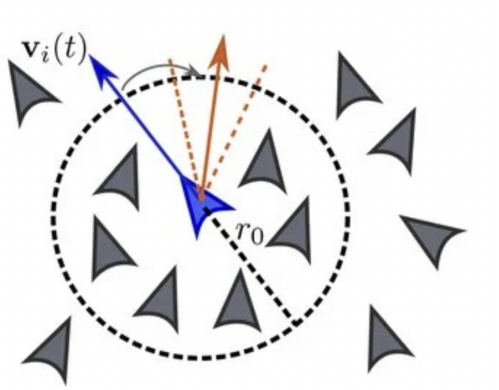

Control parameters :

noise temperature & density

$\hat{\boldsymbol{v}}_i$ similar to $\boldsymbol{s}_i$ in the Heisenberg (or XY) ferro models – though no lattice

Spontaneous symmetry breaking of polar order $\boldsymbol{p}(t) = \frac{1}{N}\sum_{i=1}^{N}\hat{\boldsymbol{v}}_i(t) \neq 0$ even in $2d$

Vicsek, Czirók, Ben-Jacob, Cohen, Shochet 95

Toner-Tu Model

Continuum model for dry active matter

Order parameter

center-of-mass velocity $\langle \boldsymbol{v} \rangle \neq 0$

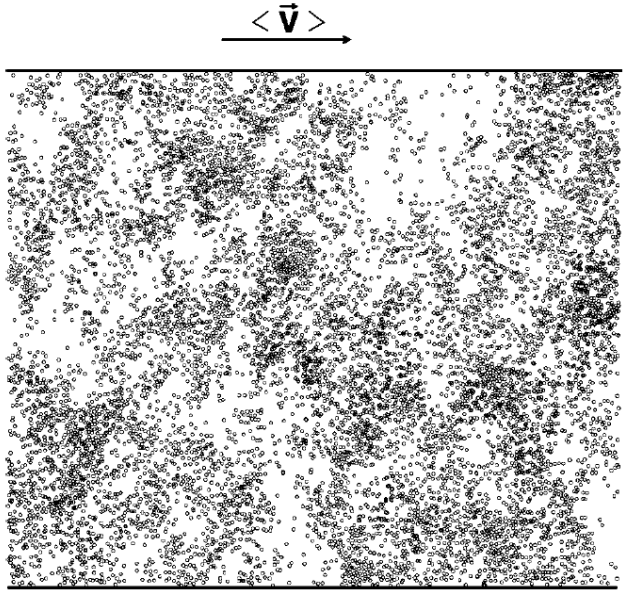

continuous rotational symmetry spont broken

Possible in low d out of equilibrium

Breakdown of linearized theory

$\Longrightarrow$ large fluctuations

Argument

Improved transport suppresses the very fluctuations that give rise to it, leading to long-range order in $d = 2$

Giant density fluctuations

Toner & Tu 95 & 98

Toner-Tu Model

Continuum model for the flock velocity field $\boldsymbol{v}(\boldsymbol{x}, t)$

$$\partial_t \boldsymbol{v} + \underbrace{\lambda_1(\boldsymbol{\nabla}\cdot\boldsymbol{v})\boldsymbol{v} + \lambda_2(\boldsymbol{v}\cdot\boldsymbol{\nabla})\boldsymbol{v} + \lambda_3\boldsymbol{\nabla}v^2}_{\text{Navier-Stokes w/no Galilean invariance}} =$$

$$\underbrace{\alpha_1\boldsymbol{v} - \alpha_2 v^2\boldsymbol{v}}_{\text{“Potential force” imposing } v^2=\alpha_1/\alpha_2} \qquad \underbrace{-\boldsymbol{\nabla}P}_{\text{“Pressure variation”}}$$

$$\underbrace{+D_B\boldsymbol{\nabla}(\boldsymbol{\nabla}\cdot\boldsymbol{v}) + D_T\nabla^2\boldsymbol{v} + D_2(\boldsymbol{v}\cdot\boldsymbol{\nabla})^2\boldsymbol{v}}_{\text{Dissipative terms}} \underbrace{+\boldsymbol{\eta}}_{\text{Noise}}$$

$$P = \sum_{n=1}^{\infty}\sigma_n(\rho-\rho_0)^n$$ Pressure imposing $\sim$ uniform density, $\rho-\rho_0$ small

$$\partial_t\rho + \boldsymbol{\nabla}\cdot(\boldsymbol{v}\rho) = 0$$ **Toner & Tu 98**

$\alpha_1 < 0$ ($\alpha_1 > 0$) in the homogenous (flocking) phase

Dry active matter e.g. herd of wildebeest, flock of birds, bacteria on agar plate

Momentum is dissipated into the substrate

Flocking in dry active matter

Vicsek & Toner-Tu Models, self-alignment

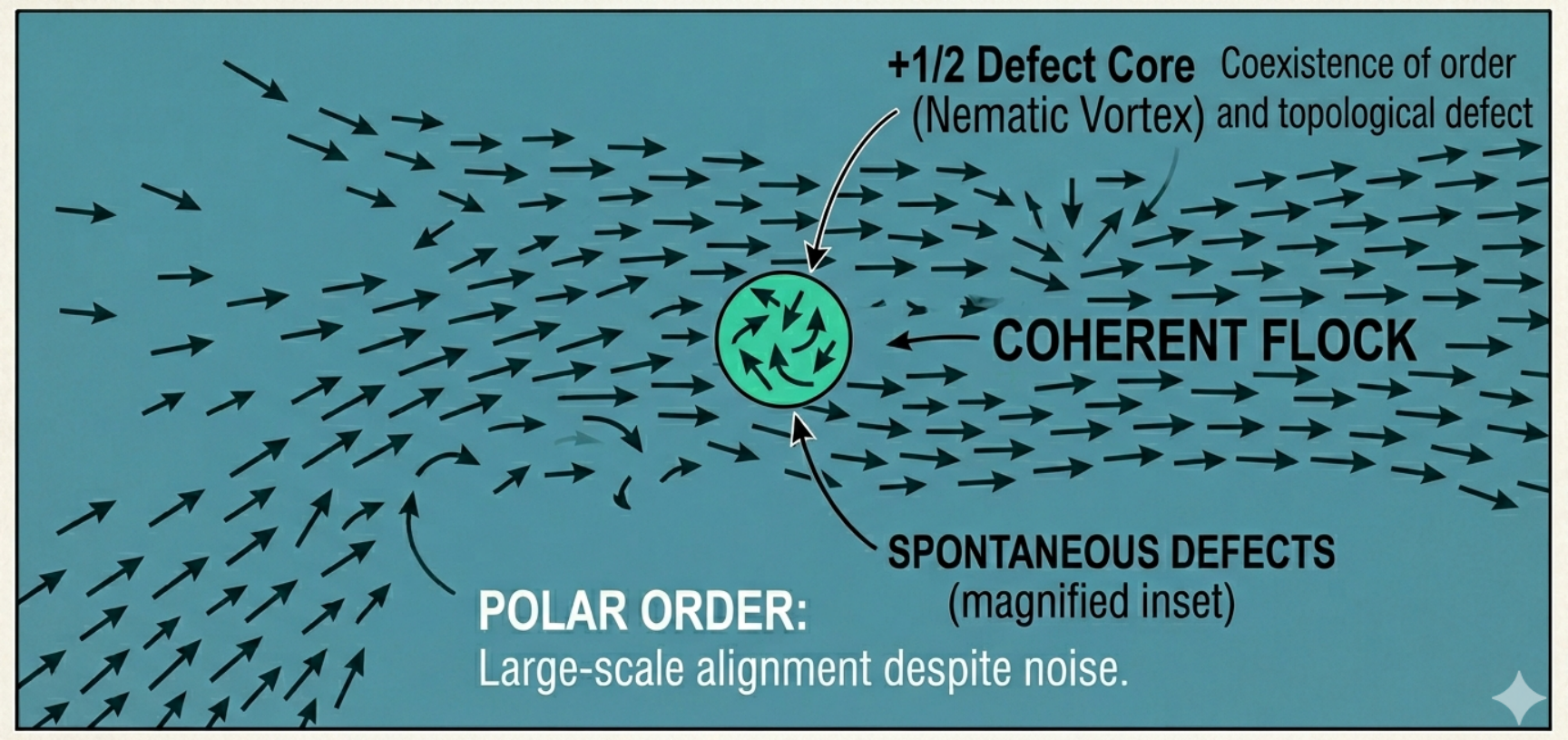

Image generated by Gemini

Flocking also in a **Hamiltonian fluid with velocity-spin coupling**

Casiulis, Tarzia, LFC & Dauchot 20

Fluctuating Hydrodynamics

Wet nematic active matter

Molecule density field c, diffusion tensor $\mathbb{D}$

Traceless & symm tensor field $\mathbb{Q}$ (head-tail symm) for orient order, γ rot friction

Fluid: velocity field $\boldsymbol{u}$, density field ρ, passive shear viscosity η, pressure P

Stress tensor $\mathbb{S} = \mathbb{S}_{\rm passive} + \mathbb{S}_{\rm active}$

with $\mathbb{S}_{\rm active} = \alpha\mathbb{Q}$, and $\alpha > 0$ for pushers and $\alpha < 0$ for pullers

$$(\partial_t + \boldsymbol{u}\cdot\boldsymbol{\nabla})\, c = \boldsymbol{\nabla}\cdot(\mathbb{D}\boldsymbol{c}) \qquad \text{mass conservation}$$

$$\rho\,(\partial_t + \boldsymbol{u}\cdot\boldsymbol{\nabla})\,\boldsymbol{u} = \eta\nabla^2\boldsymbol{u} - \boldsymbol{\nabla}P + \boldsymbol{\nabla}\mathbb{S} \qquad \text{momentum conservation}$$

$$\boldsymbol{\nabla}\cdot\boldsymbol{u} = 0 \qquad \text{incompressible fluid}$$

$$(\partial_t + \boldsymbol{u}\cdot\boldsymbol{\nabla})\,\mathbb{Q} = -\frac{1}{\gamma_{\mathbb{Q}}}\frac{\delta F}{\delta\mathbb{Q}} + \mathbb{F}(\boldsymbol{\nabla}\boldsymbol{u},\mathbb{Q}) + \boldsymbol{\eta}_{\mathbb{Q}} \qquad \text{fluid-molecule coupling}$$

e.g., suspension of cytoskeletal filaments or elongated swimming bacteria, and **active turbulence**

Marchetti, Joanny, Ramaswamy, Liverpool, Prost, Rao & Simha 13

Wet Polar/Nematic Active Matter

Fluctuating Hydrodynamics

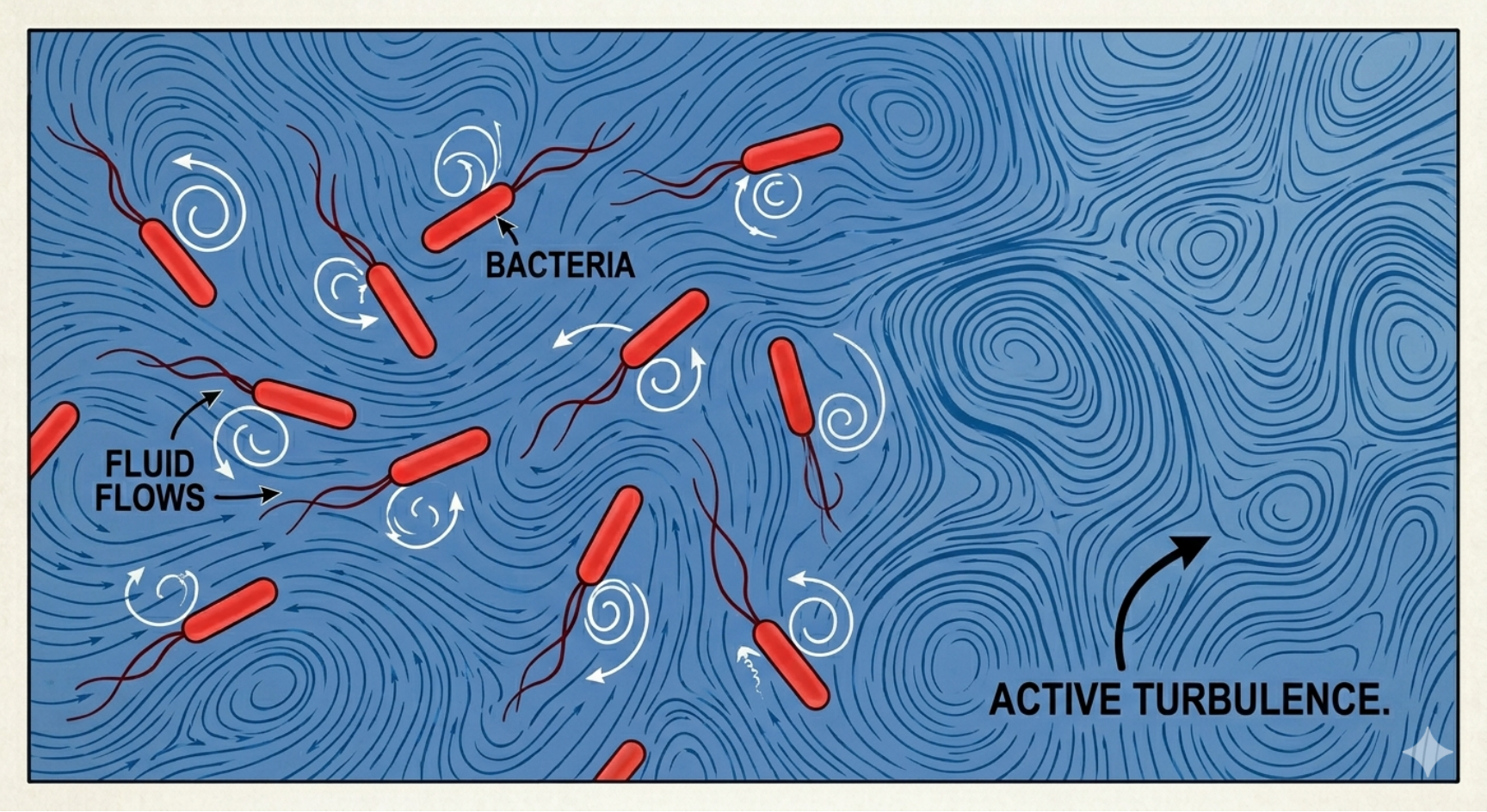

Image generated by Gemini

Active Brownian Spheres

The standard model – ABPs

Spherical particles with diameter σ_d

Environment $\Longrightarrow$ Langevin dynamics

Scales $\Longrightarrow$ over-damped motion

Self-propulsion $\Longrightarrow$ active force $\boldsymbol{F}_{\rm act}$ along $\hat{\boldsymbol{n}}_i = (\cos\theta_i(t), \sin\theta_i(t))$

$$\underbrace{\gamma \dot{\boldsymbol{r}}_i}_{\text{friction}} = \underbrace{F_{\rm act}\hat{\boldsymbol{n}}_i}_{\text{propulsion}} \underbrace{- \boldsymbol{\nabla}_i \sum_{j(\neq i)} U(r_{ij})}_{\text{inter-particle repulsion}} + \underbrace{\boldsymbol{\xi}_i}_{\substack{\text{translational}\\ \text{white noise}}} \qquad \underbrace{\dot{\theta}_i = \eta_i}_{\substack{\text{rotational}\\ \text{white noise}}}$$

$2d$ packing fraction $\boxed{\phi = \pi\sigma_d^2 N/(4S)}$ Péclet number $\boxed{\text{Pe} = F_{\rm act}\sigma_{\rm d}/(k_B T)}$

Bialké, Speck & Löwen 12, Fily & Marchetti 12

Active Models B & H

à la Ginzburg-Landau, also for, e.g., Janus particles

Scalar order parameter locally conserved

Cahn-Hilliard – Model B for phase separation

Continuity equation $\partial_t \phi(\boldsymbol{x},t) = \boldsymbol{\nabla}\cdot\boldsymbol{J}(\boldsymbol{x},t)$ with current

Active Model B

$$\boldsymbol{J}(\boldsymbol{x},t) = \underbrace{-\boldsymbol{\nabla}\frac{\delta F[\phi]}{\delta\phi(\boldsymbol{x},t)}}_{\text{equilibrium forcing}} \underbrace{-\boldsymbol{\nabla}\lambda[\boldsymbol{\nabla}\phi(\boldsymbol{x},t)]^2}_{\text{non-eq} \neq -\boldsymbol{\nabla}\delta F/\delta\phi} + \underbrace{\boldsymbol{\eta}(\boldsymbol{x},t)}_{\text{noise}}$$

Active Model B+

$$\boldsymbol{J} \mapsto \boldsymbol{J} + \underbrace{\zeta(\nabla^2\phi)\boldsymbol{\nabla}\phi - \frac{1}{2}\boldsymbol{\nabla}(\boldsymbol{\nabla}\phi)^2}_{\text{high-order terms order } \nabla^3 \text{ and } \phi^2}$$

Active Model H with hydrodynamics as well

Focus on Active Brownian Particles

2d Active Matter

Why two dimensions ?

It is **experimentally** 'easier' than three dimensions

It is computationally lighter to **simulate** $2d$ systems than $3d$ ones

It is already **very rich** and **often realistic**

Focus here on two kinds of active constituents

Disks

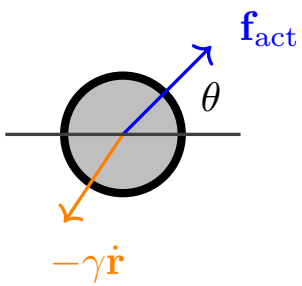

Rigid Dumbbells

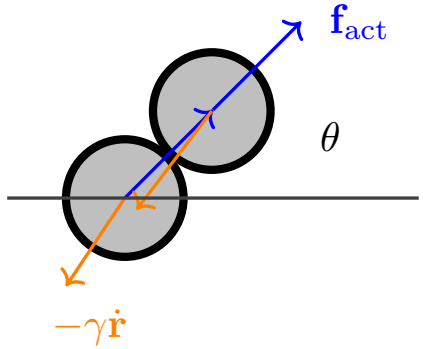

Space dimension

Two dimensions is special

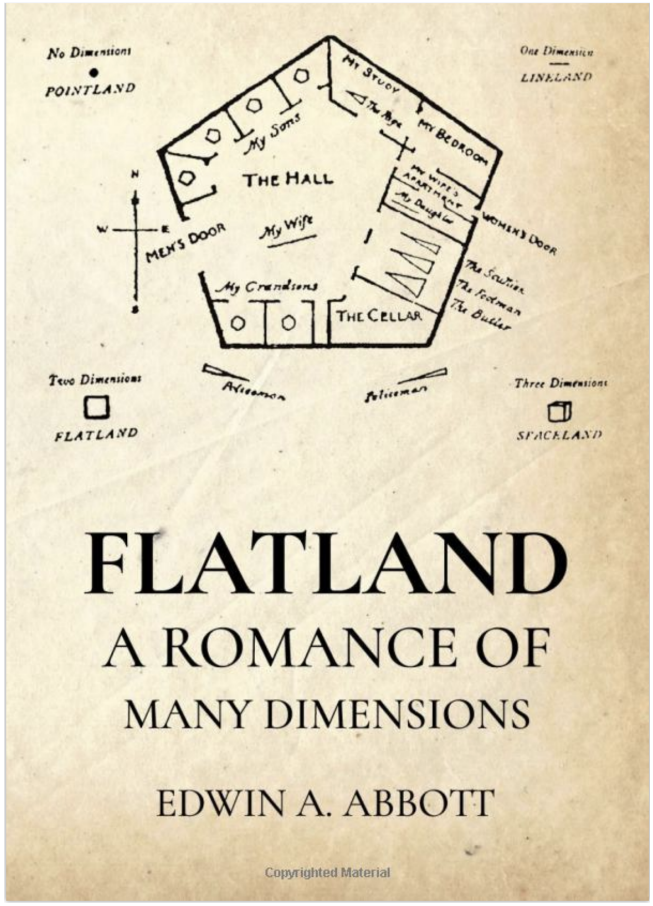

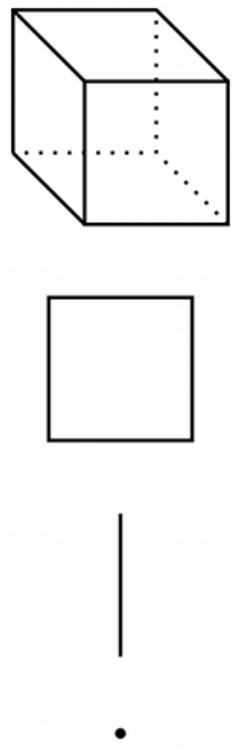

$d = 3$

$d = 2$

$d = 1$

$d = 0$

Active Brownian Matter

Questions – à la Statistical Physics – on bidimensional systems

- Activity (Pe) - packing fraction (ϕ) phase diagram.
- Order of, and mechanisms for, the phase transitions.
  - Correlations, fluctuations.
  - Topological defects.

- Motility Induced Phase Separation.
  - Internal structure of the dense phase.
  - Mechanisms for growth of the dense phase.
    - Influence of particle shape, *e.g.* disks *vs.* dumbbells.

Active Brownian DIsks

Out of equilibrium phase diagram - Collective behaviour

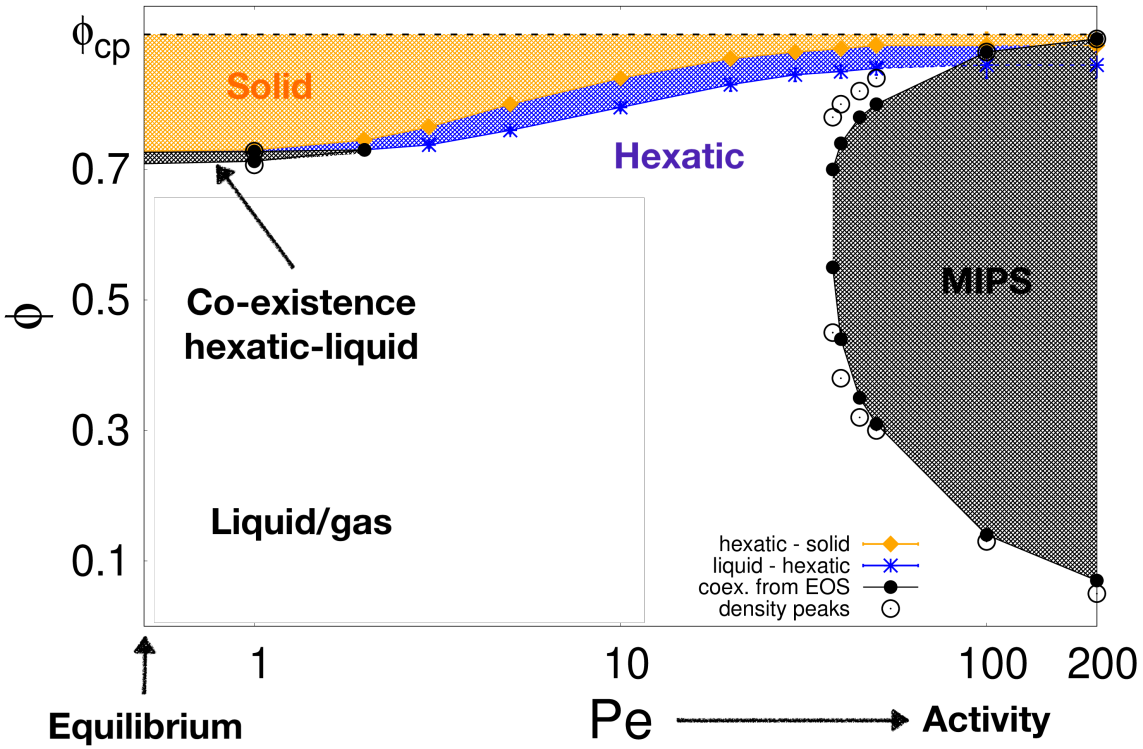

Gray zone at high Pe

Motility induced

phase separation (MIPS)

gas & dense

Cates & Tailleur 15

Farage, Krinninger & Brader 15

Pressure $P(\phi, \mathrm{Pe})$ (EOS), correlations $G_T(r)$, $G_6(r)$, and distributions of ϕ_i, $|\psi_{6i}|$

Digregorio, Levis, Suma, LFC, Gonnella & Pagonabarraga 18

Freezing/Melting in 2d

Freezing/Melting

Different routes in $3d$ and $2d$

$T = 0$

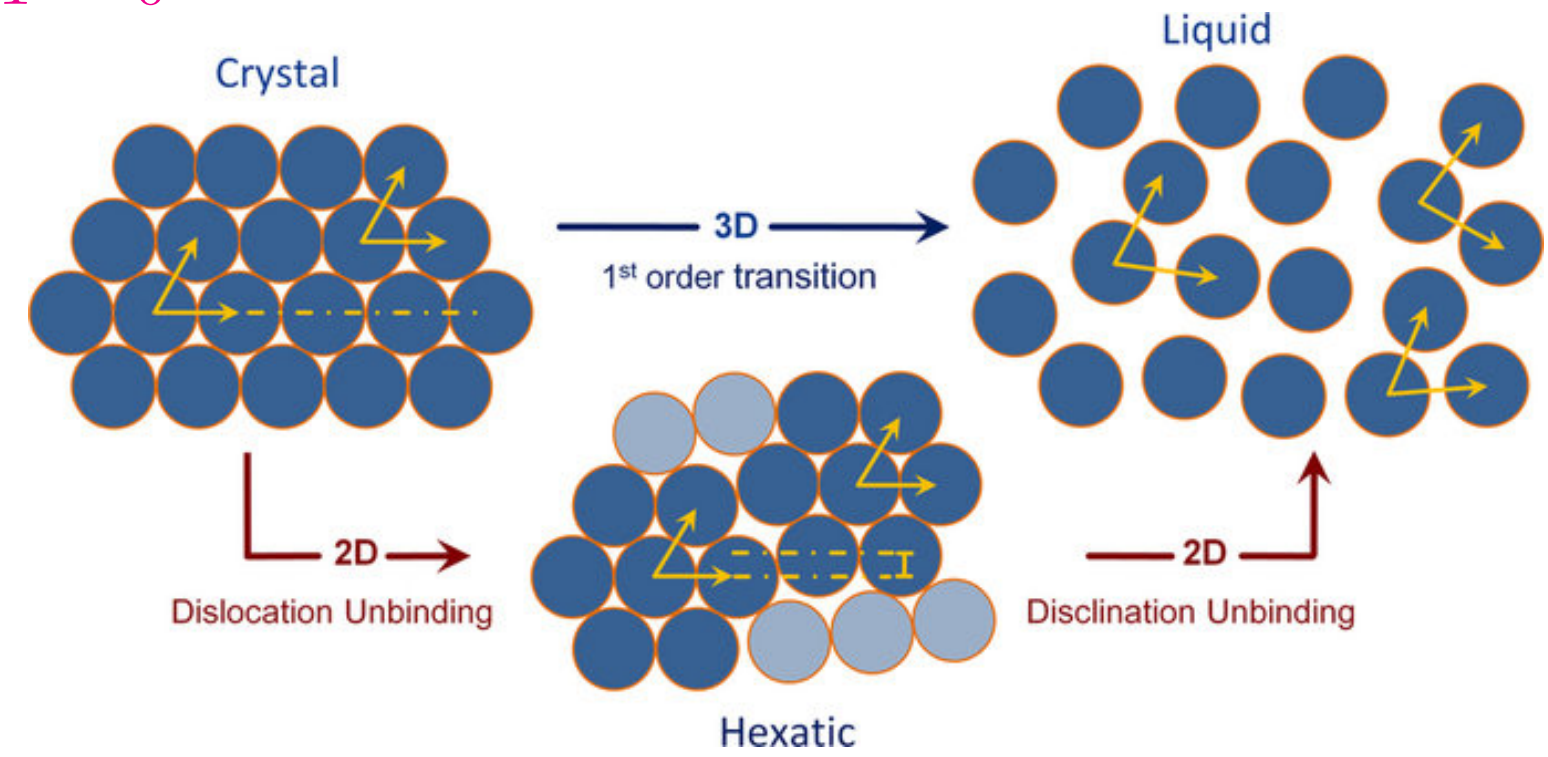

Orientation order preserved also lost

Image from **Pal, Kamal & Raghunathan 16**

Measures of

Translational & orientational order

Positional order

Translational order

The (fluctuating) **local particle number density** is

$$\rho(\boldsymbol{r}_0) \equiv \sum_{i=1}^{N} \delta(\boldsymbol{r}_0 - \boldsymbol{r}_i) \qquad\qquad \tilde{\rho}(\boldsymbol{q}) = \sum_{j=1}^{N} e^{\mathrm{i}\boldsymbol{q}\cdot\boldsymbol{r}_j}$$

with $\int d^d\boldsymbol{r}_0\, \rho(\boldsymbol{r}_0) = N$. In an homogeneous system $\rho(\boldsymbol{r}_0) = N/V = \overline{\rho}$

The **structure factor**

$$S(\boldsymbol{q}) = \tfrac{1}{N}\langle \sum_{ij} e^{-\mathrm{i}\boldsymbol{q}\cdot(\boldsymbol{r}_i - \boldsymbol{r}_j)} \rangle = 1 + \overline{\rho} \int d^d\boldsymbol{r}\, [g(r) - 1]\, e^{\mathrm{i}\boldsymbol{q}\cdot\boldsymbol{r}}$$

Isotropic system, $S(\boldsymbol{q}) \mapsto S(q)$

The 1st peak in $S(q)$ is at $q_0 = 2\pi/\Delta r$ where $\Delta r \sim$ inter particle distance

$$G_{\boldsymbol{q}_0}(r) = \langle \sum_{ij} e^{\mathrm{i}\boldsymbol{q}_0\cdot(\boldsymbol{r}_i - \boldsymbol{r}_j)} \rangle \Big|_{\boldsymbol{r}_i - \boldsymbol{r}_j = \boldsymbol{r}} = \langle \sum_{ij} \cos[\boldsymbol{q}_0 \cdot (\boldsymbol{r}_i - \boldsymbol{r}_j)] \rangle \Big|_{\boldsymbol{r}_i - \boldsymbol{r}_j = \boldsymbol{r}}$$

Voronoi tessellation

Notion of neighborhood

A Voronoi diagram is induced by a set of points, called sites, that in our case are the centres of the dumbbell beads.

The plane is subdivided into faces that correspond to the regions where one site is closest.

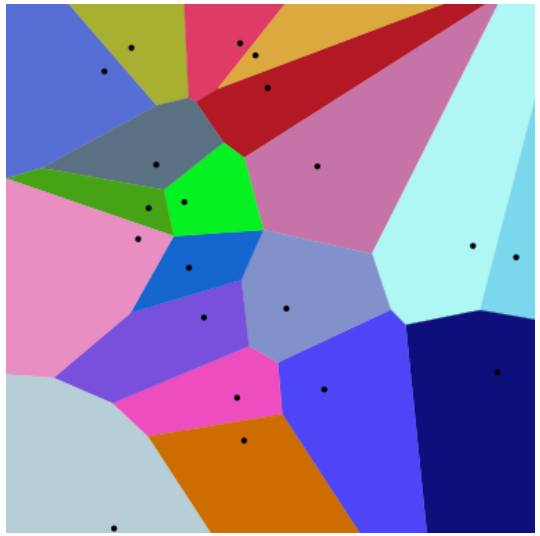

Focus on the central light-green face

All points within this region are closer to the dot within it than to any other dot on the plane

The region has five neighbouring cells from which it is separated by an edge

The grey zone has six neighbouring cells

Orientational Order

Hexatic (similarity with an hexagonal lattice)

The **local hexatic fluctuating order**

$$\psi_{6j} = \frac{1}{N_{\rm nn}^{(j)}} \sum_{k=1}^{N_{\rm nn}^{(j)}} e^{6{\rm i}\theta_{jk}}$$

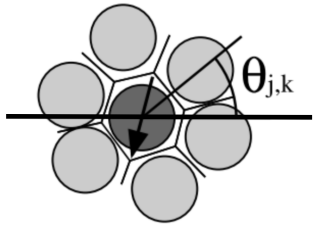

with $N_{\rm nn}^{(j)}$ the number of nearest (Voronoi) neighbours of bead j and θ_{jk} the angle between the segment that connects j with its neighbour k and the x axis.

For beads placed on the vertices of a triangular/hexagonal lattice, aligned w/x, each bead has six nn, $k = 1, \ldots, 6$, the angles are $\theta_{jk} = 2\pi k/6$ and $\psi_{6j} = 1$ for all j

Correlation function

$$G_6(r) = \frac{\sum_{ij} \left[\langle \psi_{6i}^* \psi_{6j} \rangle\right]\big|_{r_{ij}=r}}{\left[\langle |\psi_{6i}|^2 \rangle\right]}$$

normalisation is site independent

Correlations & defects

Hexatic **Positional** **• 7 neighb** **• 5 neighb**

Solid Hexatic Liquid

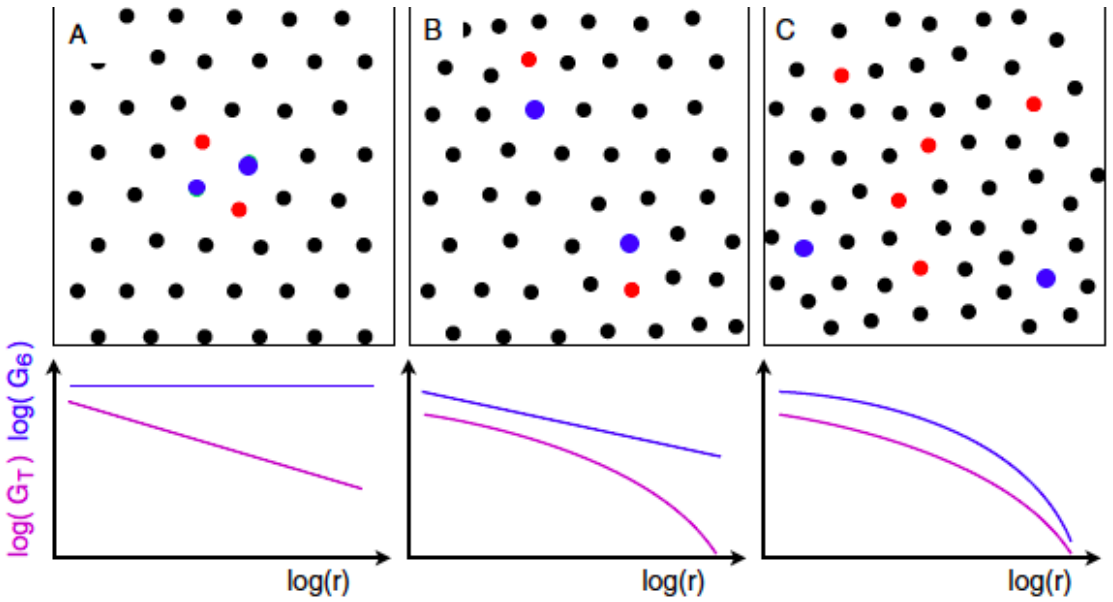

T or $1/\phi$

long r: $G_6(r) = \begin{cases} \text{cst} & \text{solid} & \text{long range order} \\ r^{-\eta_6} & \text{hexatic} & \text{quasi long range order} \\ e^{-r/\xi_6} & \text{liquid} & \text{disorder} \end{cases}$

Correlations & defects

Hexatic **Positional** **• 7 neighb** **• 5 neighb**

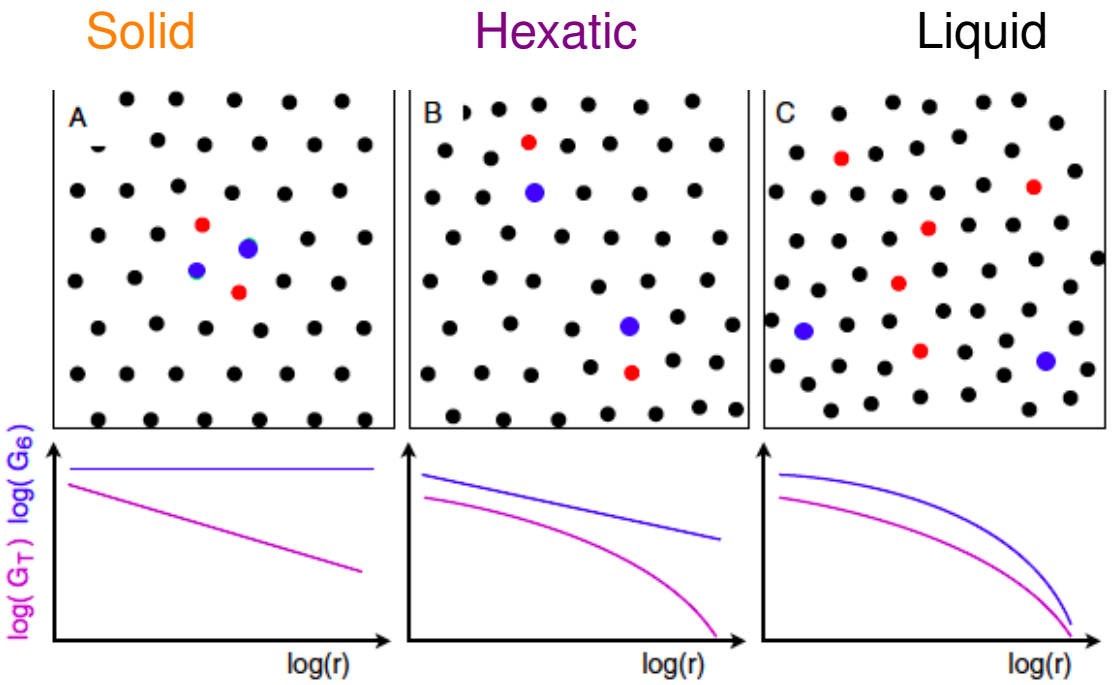

T or $1/\phi$

long r: $G_{\boldsymbol{q}_0}(r) = \begin{cases} r^{-\eta} & \text{solid} \quad \text{quasi long range order} \\ e^{-r/\xi_h} & \text{hexatic} \quad \text{disorder} \\ e^{-r/\xi_l} & \text{liquid} \quad \text{disorder} \end{cases}$

Phases & transitions

Berezinskii, Kosterlitz, Thouless, Halperin, Nelson & Young 70s

	BKT-HNY
Solid	QLR positional & LR orientational
transition	BKT (unbinding of dislocations)
Hexatic phase	SR positional & QLR orientational
transition	BKT (unbinding of disclinations)
Liquid	SR positional & orientational

Two infinite order, $\xi \propto e^{\delta^{-\nu}}$ for $\delta \to 0$,

Berenzinskii, Kosterlitz & Thouless

transitions

Phase Diagram

Solid, hexatic, liquid, co-existence and MIPS

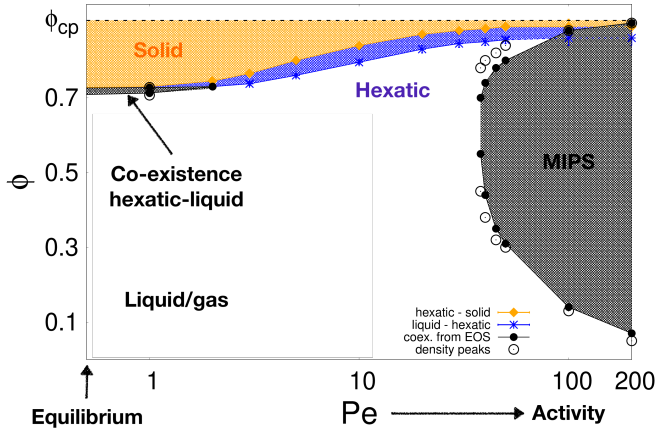

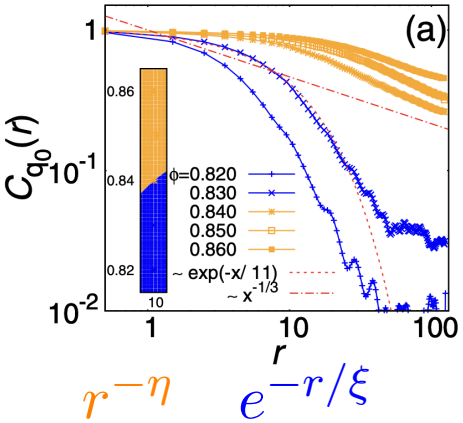

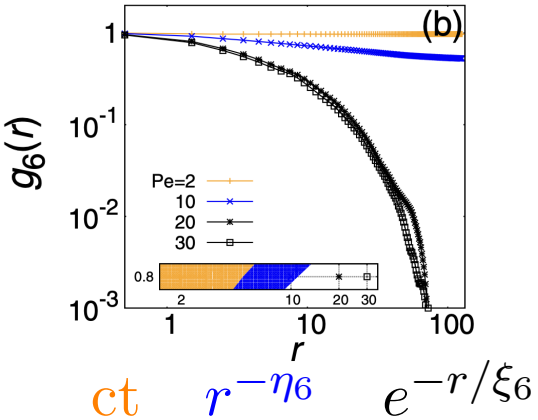

Phases characterized by

– Translational correlations $G_{\boldsymbol{q}_0}(r)$ & orientational order correlations $G_6(r)$

$G_{\boldsymbol{q}_0}$ algebraic in **solid**
$G_{\boldsymbol{q}_0}$ exponential in **hexatic**
$G_{\boldsymbol{q}_0}$ exponential in **liquid**

G_6 no decay **solid**
G_6 power law in **hexatic**
G_6 exponential in **liquid**

Digregorio, Levis, Suma, LFC, Gonnella & Pagonabarraga 18

Active Brownian disks

Phase diagram with solid, hexatic, liquid, co-existence and MIPS

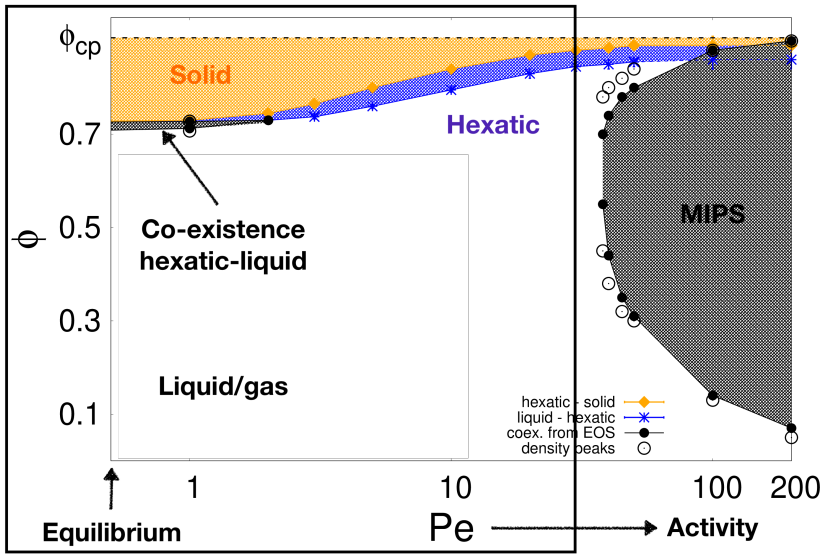

However

Different from BKTHNY picture

1st order **hexatic**-**liquid** close to Pe = 0

KT-HNY **solid**-**hexatic** dislocation unbinding

Pressure $P(\phi, \mathrm{Pe})$ (EOS), correlations $G_{\boldsymbol{q}_0}(r)$, $G_6(r)$, and distributions of ϕ_i, $|\psi_{6i}|$

defect identification & counting

Digregorio, Levis, Suma, LFC, Gonnella & Pagonabarraga 18

Bernard & Krauth 11, Kapfer & Krauth 16, Klamser, Kapfer & Krauth 18

Passive hard disks

Phase diagram

$\phi_{\mathrm{CP}} \uparrow$

ϕ

$\phi_{\mathrm{RCP}} \uparrow$

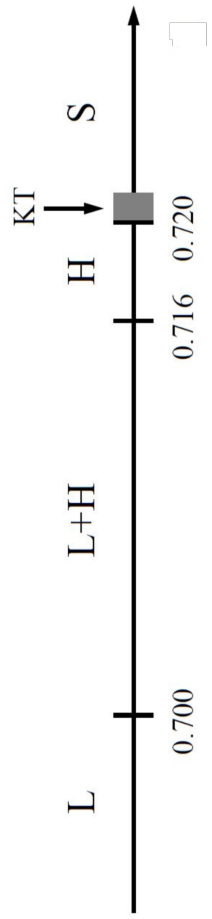

solid

hexatic

co-existence

liquid

$n = 32, T = 0.05, \gamma = 10, m = 1, \sigma_d = 1, \tau_p = 60, N \sim 10^6$

MareNostrum (Barcelona, España) & Galileo (Cineca, Italia) computer facilities

Passive hard disks

Local density & local hexatic parameter

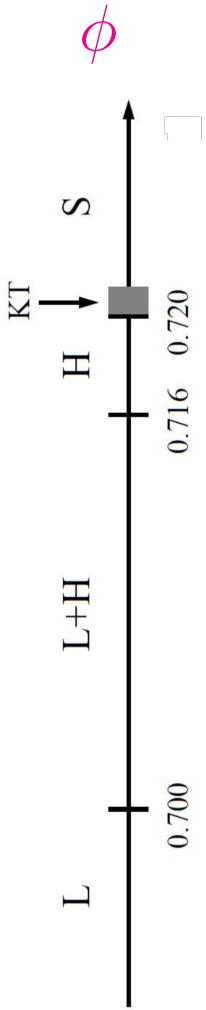

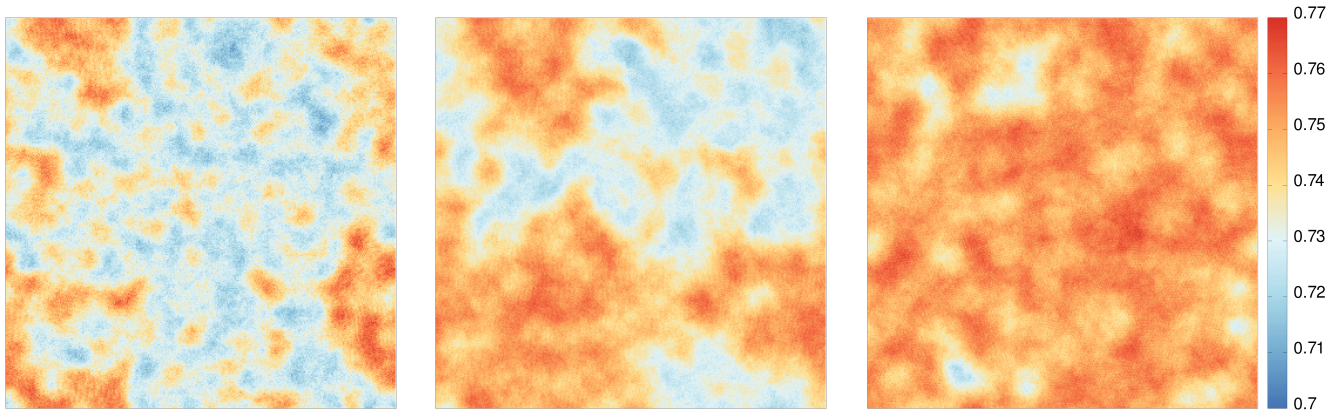

(co-existence) (co-existence) (upper limit of co-existence)

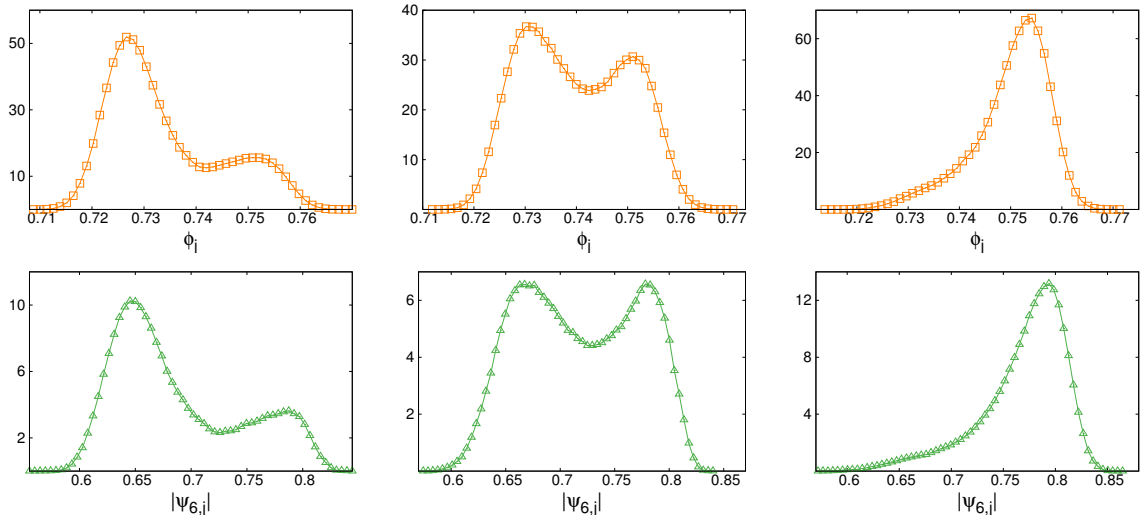

Liquid **Hexatic**

Active hard disks

Distribution of the local density

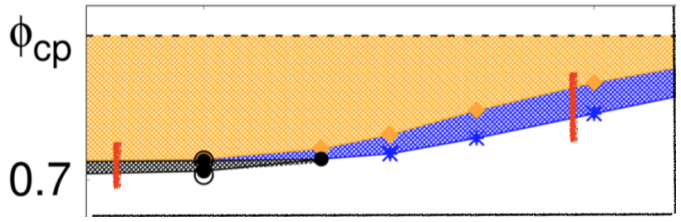

Pe = 1

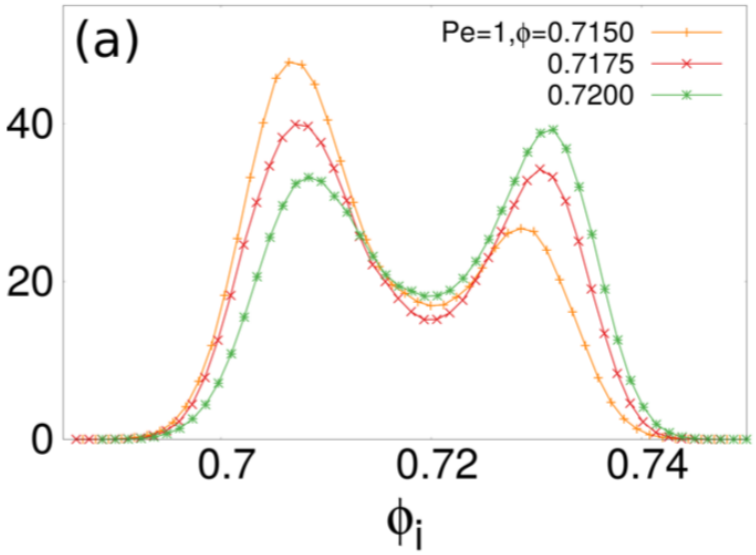

First order - coexistence

Pe = 10

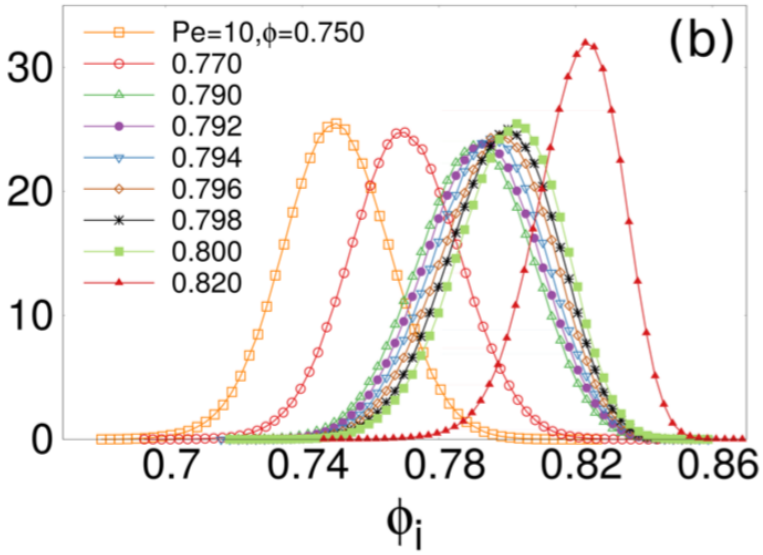

Continuous transition

Phases & transitions

BKT-HNY *vs.* a new scenario by Bernard & Krauth 2011

	BKT-HNY	BK
Solid	QLR pos & LR orient	QLR pos & LR orient
transition	BKT (unbinding of dislocations)	BKT
Hexatic phase	SR pos & QLR orient	SR pos & QLR orient
transition	BKT (unbinding of disclinations)	**1st order**
Liquid	SR pos & orient	SR pos & orient

Basically, the phases are the same, but the **hexatic**-**liquid** transition is different, allowing for **coexistence of the two phases** for **hard enough particles**

Event driven MC simulations. Sketches from **Bernard's** thesis.

Active Brownian disks

Phase diagram with solid, hexatic, liquid, co-existence and MIPS

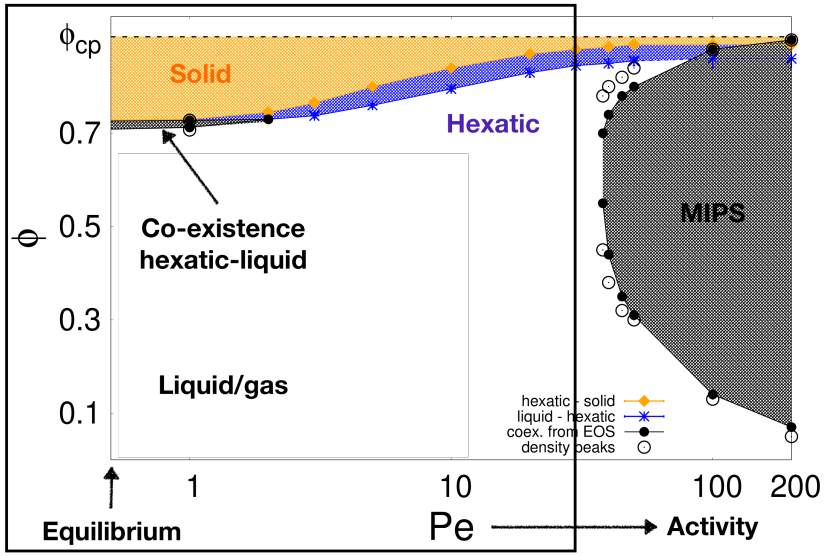

Different from BKTHNY picture

1st order **hexatic**-**liquid** close to Pe = 0

KT-HNY **solid**-**hexatic** dislocation unbinding

disclination unbinding, not really the drive

percolation of defect clusters in liquid

Pressure $P(\phi, \mathrm{Pe})$ (EOS), correlations $G_{\boldsymbol{q}_0}(r)$, $G_6(r)$, and distributions of ϕ_i, $|\psi_{6i}|$

defect identification & counting

Analysis of defects

What drives the phase transitions ?

Highlighted the particles with 5 & 7 neighbours

Topological Defects

Close packing of disks

Disks, Voronoi cells & dislocations

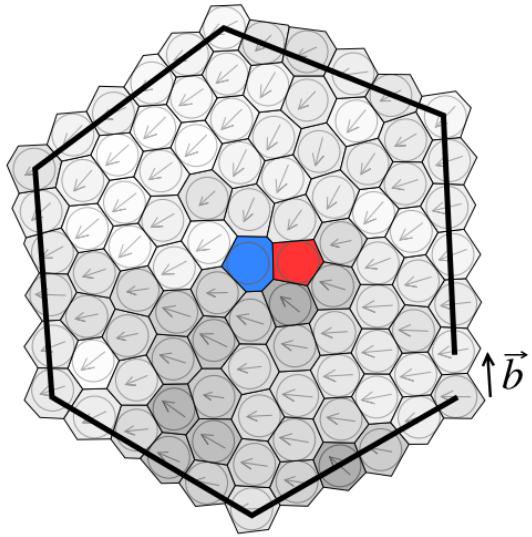

A free dislocation

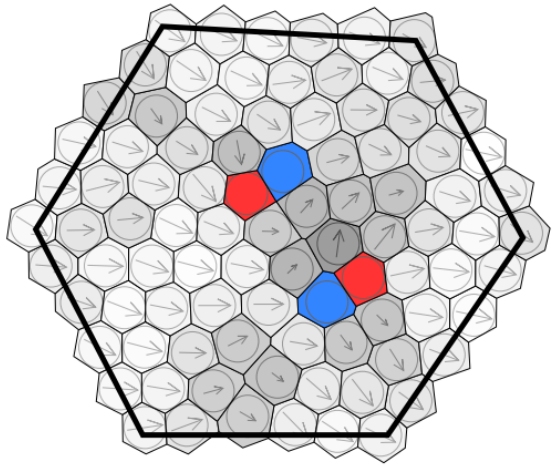

A bound pair of dislocations

In the crystal the centers of the disks form a triangular lattice

The **blue** disks have seven neighbours and the **red** ones have five.

On the right image: the external path closes and forms a perfect hexagon.

The effects of the defects are confined. This is the **solid** phase.

Close packing of disks

Disks, Voronoi cells & dislocations

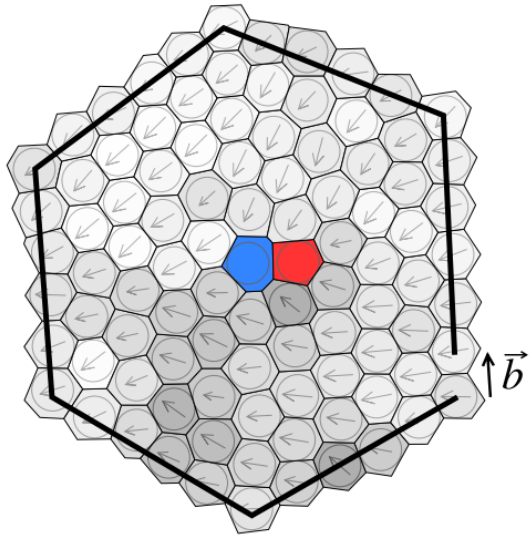

A free dislocation

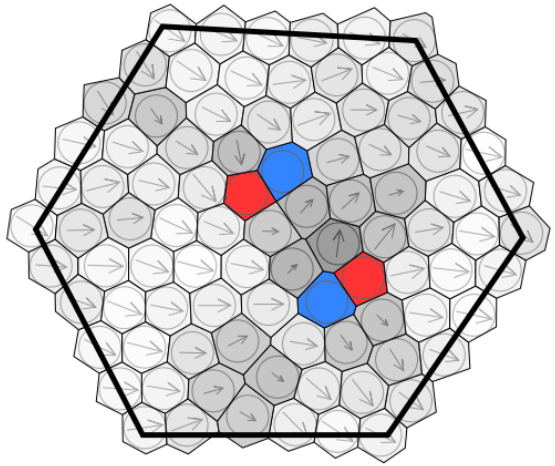

A bound pair of dislocations

In the crystal the centres of the disks form a triangular lattice

The **blue** disks have seven neighbours and the **red** ones have five.

On the left image: the external path fails to close, no perfect hexagon. The effect of the defects spreads & kills translation order: **hexatic** phase.

Close packing of disks

Unbinding of disclinations

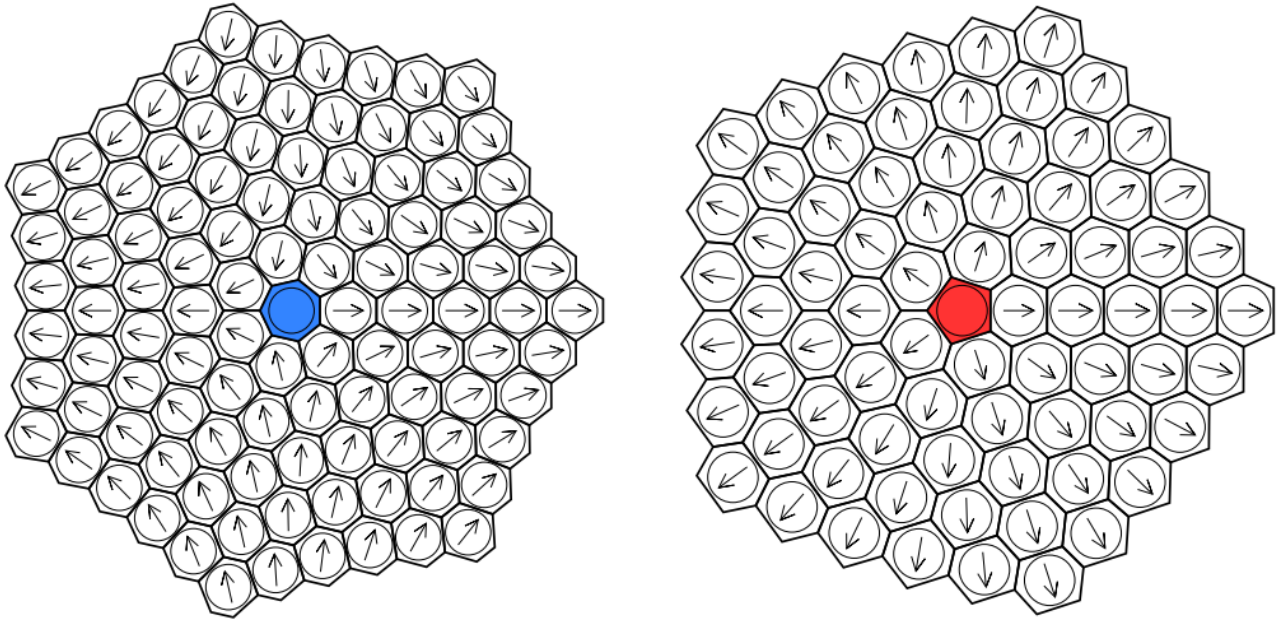

The orientation winds by $\pm 2\pi$ around the **blue** (seven) and **red** (five) defects.

Very similar to the vortices in the $2d$ XY magnetic model.

Halperin, Nelson & Young scenario: the unbinding of disclinations drives a second BKT-like transition to the **liquid**.

What happens with the defects ?

Defects & grain boundaries

Classification

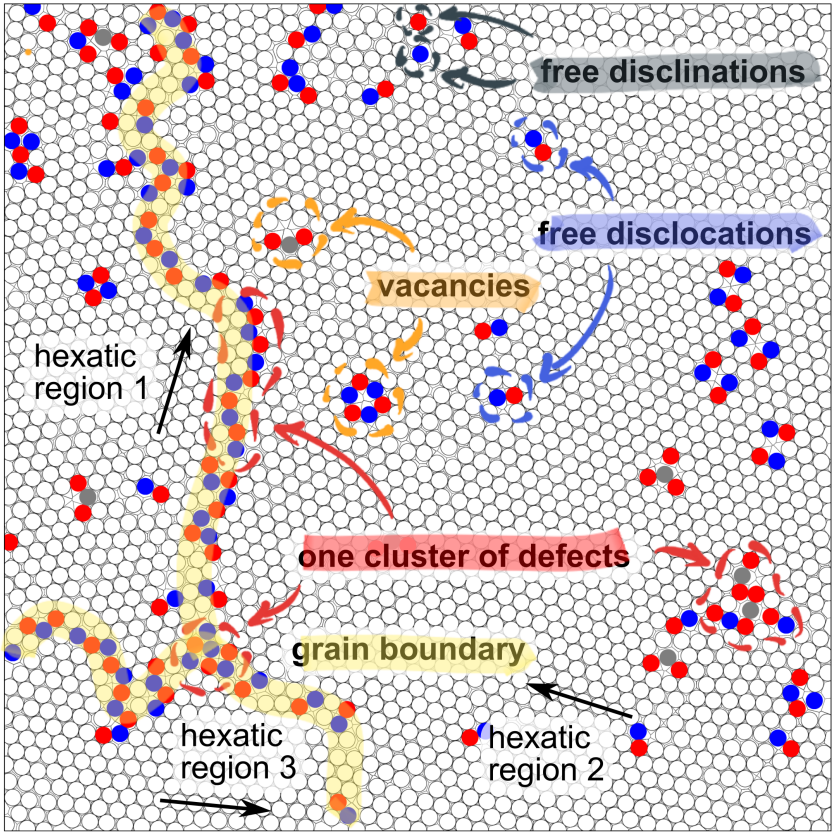

The classification in **Pertsinidis & Ling 01**

Unbinding of defects

Solid-hexatic transition & the emergence of the liquid at Pe = 0

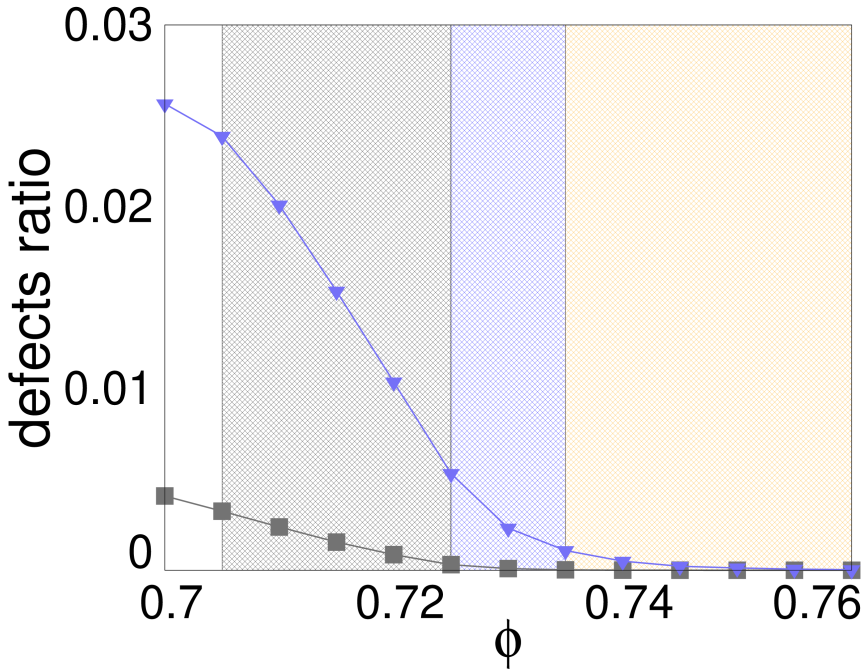

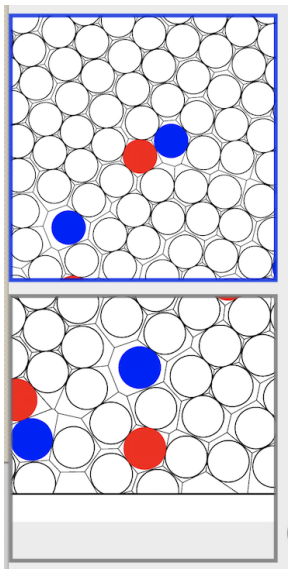

Dislocations ▼

Disclinations ■

Dislocations ▼ unbind at the **solid** - **hexatic** transition as in BKT-HNY

Disclinations ■ unbind when the liquid appears in the co-existence region

Digregorio, Levis, LFC, Gonnella & Pagonabarraga 22

Unbinding of Dislocations

At the solid-hexatic transition at Pe = 0

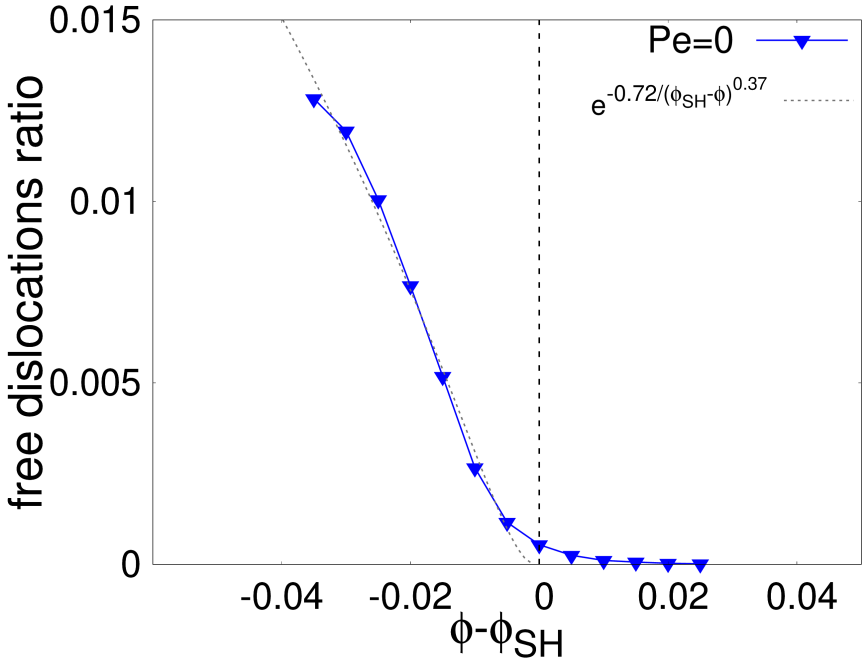

Dislocations ▼ unbind at the **solid** - **hexatic** transition $\phi_{\mathrm{sol-hex}}$

Measured exponent $\nu_{\mathrm{sol-hex}} \approx 0.37$ independently of Pe

Digregorio, Levis, LFC, Gonnella & Pagonabarraga 22

Han, Ha, Alsayed, & Yodh 08

Solid-Hexatic Transition

Universality

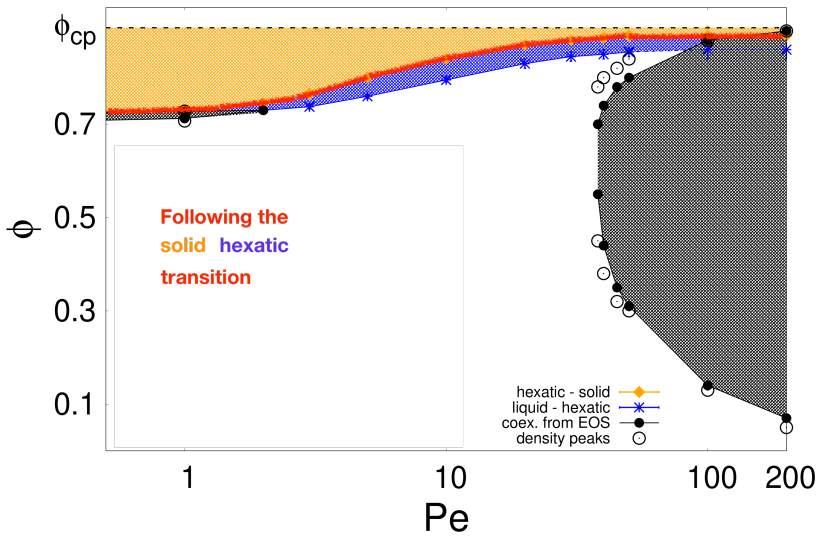

Free dislocation:
a 7-5 neighbor

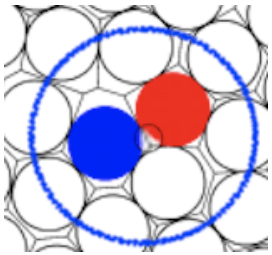

$\neq$ from $\triangle$ lattice

Solid - **Hexatic** transition $\phi_{\mathrm{sol-hex}}$, **driven by unbinding of dislocation pairs as in Berezinskii-Kosterlitz-Thouless-Halperin-Nelson-Young universality ?**

$$\rho_{\mathrm{disloc}} \simeq a \, \exp\left[-b\left(\frac{\phi_{\mathrm{sol-hex}}}{\phi_{\mathrm{sol-hex}}-\phi}\right)^{\nu}\right] \qquad \nu \sim 0.37 \;\; \forall \mathrm{Pe}$$

Digregorio, Levis, LFC, Gonnella & Pagonabarraga 22

Solid-Hexatic Transition

Universality ?

Positional correlation function on the **solid**-**hexatic** critical line $\phi_{\mathrm{sol-hex}}$,

coming from the **solid** side

G_T

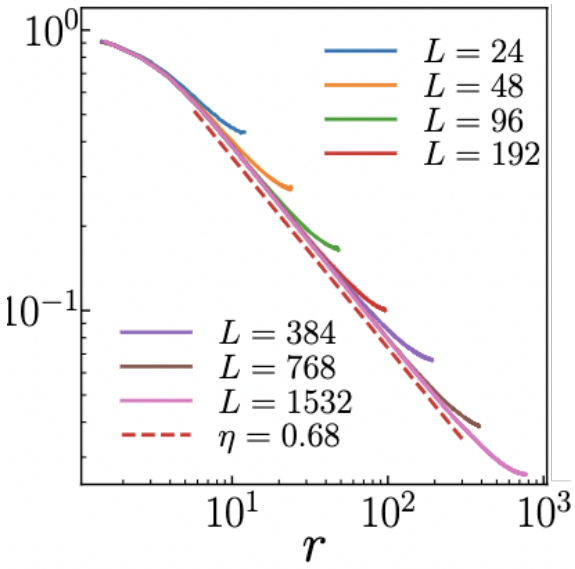

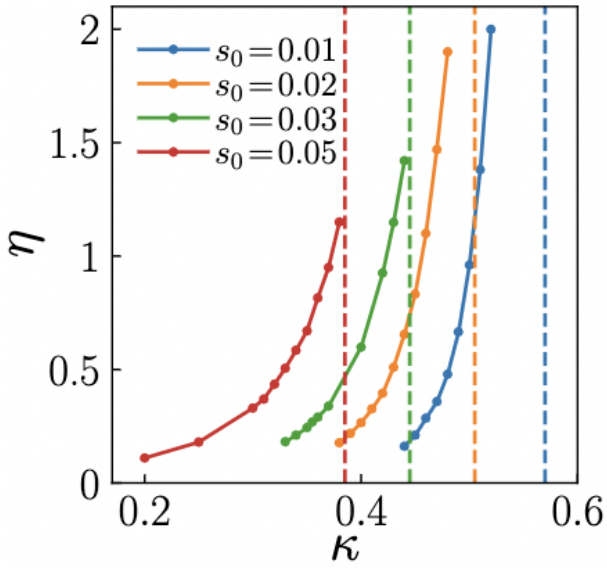

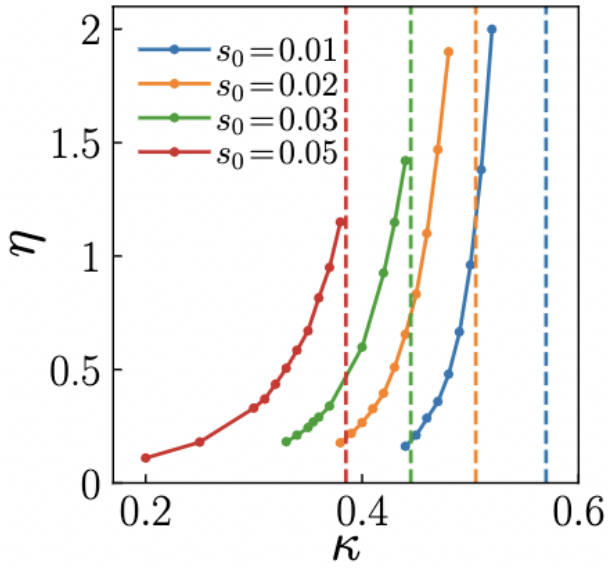

Pe

The exponent η varies along the transition line while ν does not

Shi, Cheng & Chaté 23

Digregorio, LFC & Gonnella, in preparation

Disclinations

At the hexatic - liquid transition $\phi_{\mathrm{hex-liq}}$ at all Pe

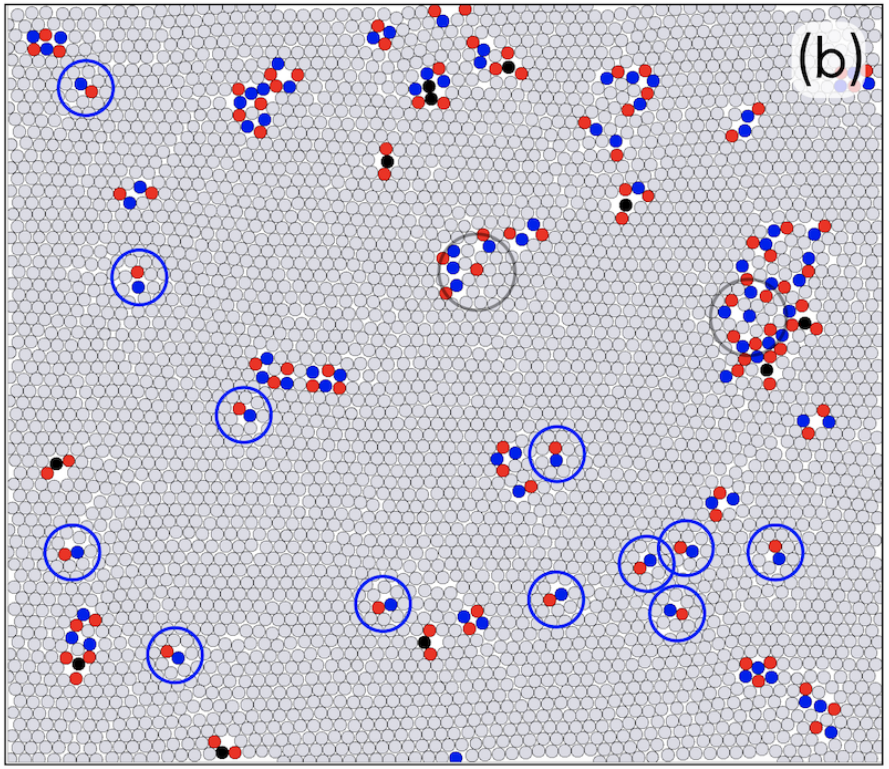

dislocations

disclinations

Very few disclinations, and always very close to other defects, so **not free**

Proliferation of clusters

Within the co-existence region & all along the hexatic-liquid transition

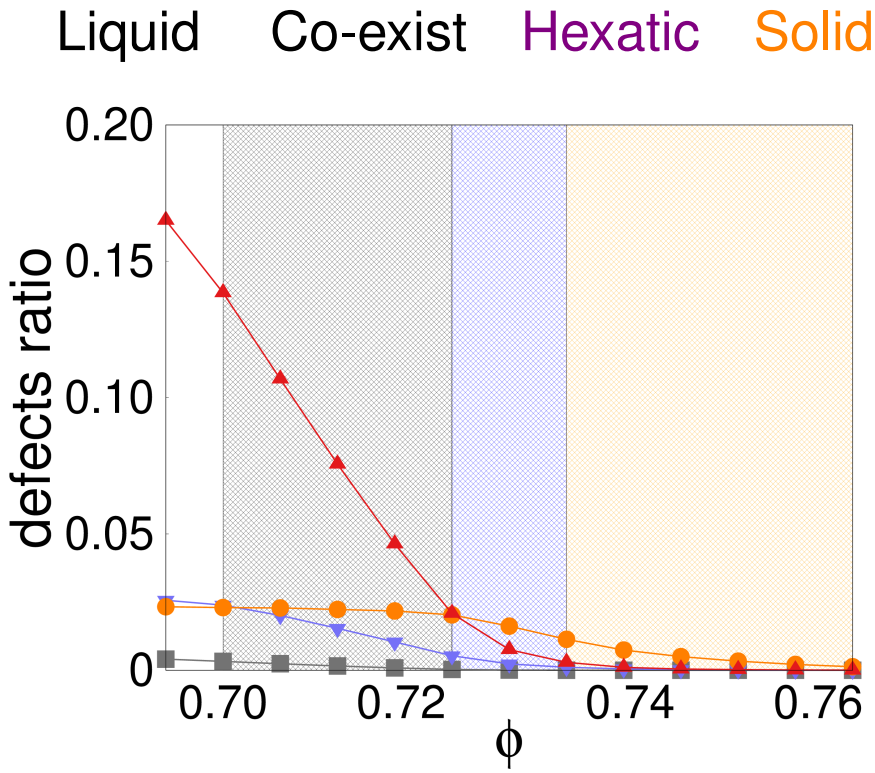

Clusters ▲ of defects proliferate within the co-existence region

Vacancies ● remain approximately constant within the co-existence region

Digregorio, Levis, LFC, Gonnella & Pagonabarraga 22

Topological defects

Summary of results

- **Solid** - **hexatic** à la BKTHNY even quantitatively (ν value) and independently of the activity (Pe) *Universality ?* *
- **Hexatic** - **liquid** very few disclinations and not even free

  Breakdown of the BKT-HNY picture for all Pe (even zero)
- Close to, but in the liquid, **percolation** of *clusters of defects* with properties of uncorrelated critical percolation (d_f, τ)
- In **MIPS**, network of defects on top of the interfaces between hexatically ordered regions, interrupted by the *gas bubbles in cavitation*

Digregorio, Levis, Cugliandolo, Gonnella & Pagonabarraga 22

*Shi, Cheng & Chaté 23 Digregorio, LFC & Gonnella in preparation

Active Brownian disks

Phase diagram with solid, hexatic, liquid, co-existence and MIPS

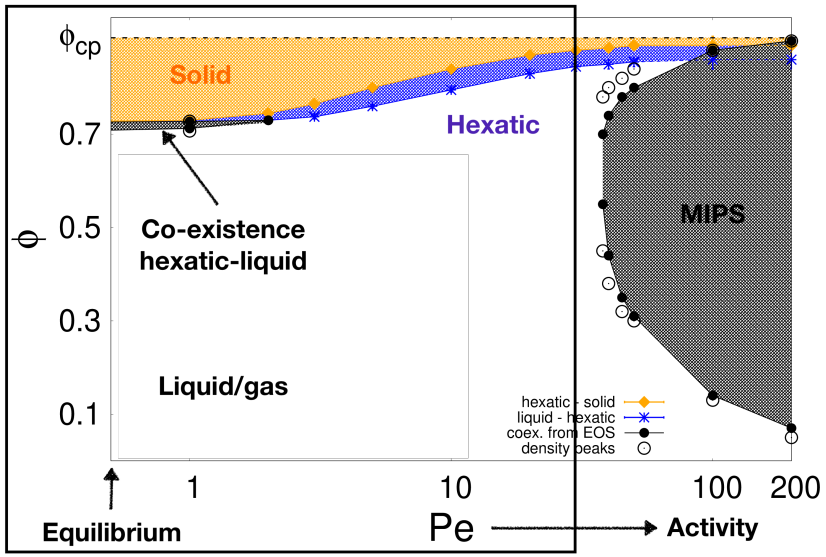

Different from BKTHNY picture

1st order **hexatic**-**liquid** close to Pe = 0

KT-HNY **solid**-**hexatic** dislocation unbinding

disclination unbinding in liquid

percolation of defect clusters in liquid

Pressure $P(\phi, \mathrm{Pe})$ (EOS), correlations $G_{\boldsymbol{q}_0}(r)$, $G_6(r)$, and distributions of ϕ_i, $|\psi_{6i}|$

defect identification & counting

Digregorio, Levis, Suma, LFC, Gonnella & Pagonabarraga 18

Klamser, Kapfer & Krauth 18

Active Brownian Matter

Questions – à la Statistical Physics – on bidimensional systems

- Activity (Pe) - packing fraction (ϕ) phase diagram.
- Order of, and mechanisms for, the phase transitions.
  - Correlations, fluctuations.
  - Topological defects.

- Motility Induced Phase Separation.
  - Internal structure of the dense phase.
  - Mechanisms for growth of the dense phase.
    - Influence of particle shape, *e.g.* disks *vs.* dumbbells.

Active Brownian disks

Phase diagram with solid, hexatic, liquid, co-existence and MIPS

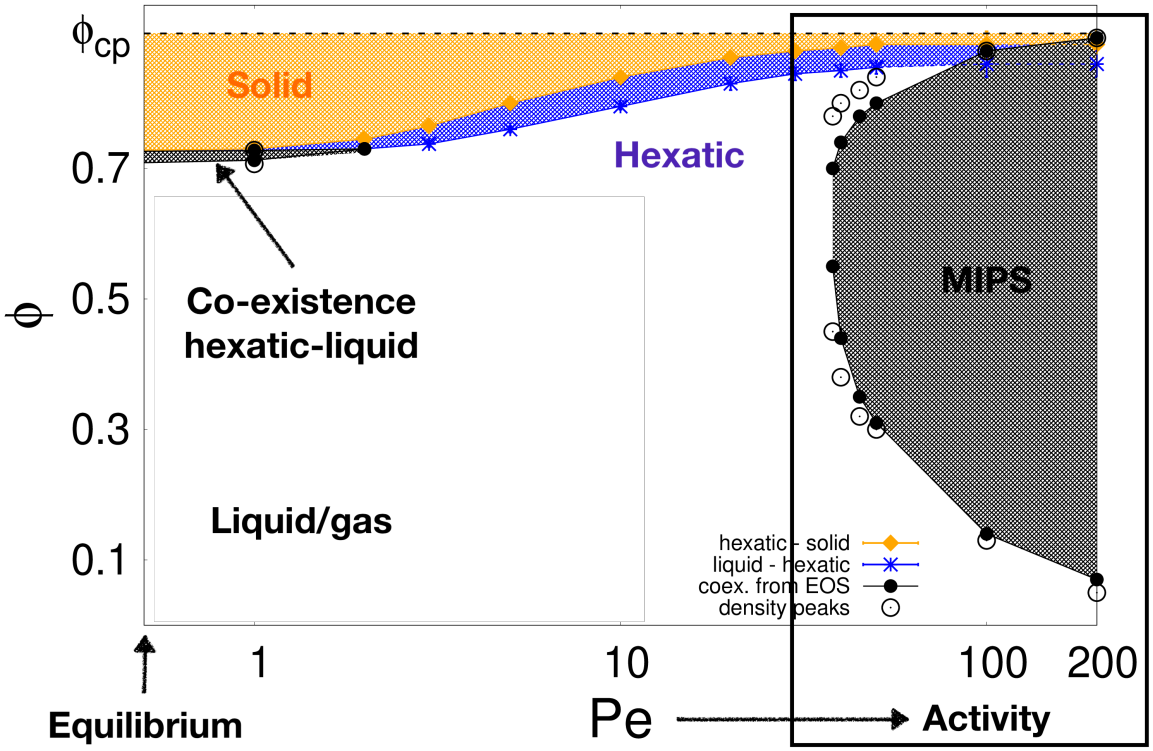

Motility induced

phase separation (MIPS)

gas & dense

Cates & Tailleur

Farage, Krinninger & Brader 15

Pressure $P(\phi, \mathrm{Pe})$ (EOS), correlations $G_T(r)$, $G_6(r)$, and distributions of ϕ_i, $|\psi_{6i}|$

Digregorio, Levis, Suma, LFC, Gonnella & Pagonabarraga 18

MIPS

Active Brownian Particles & Model B+

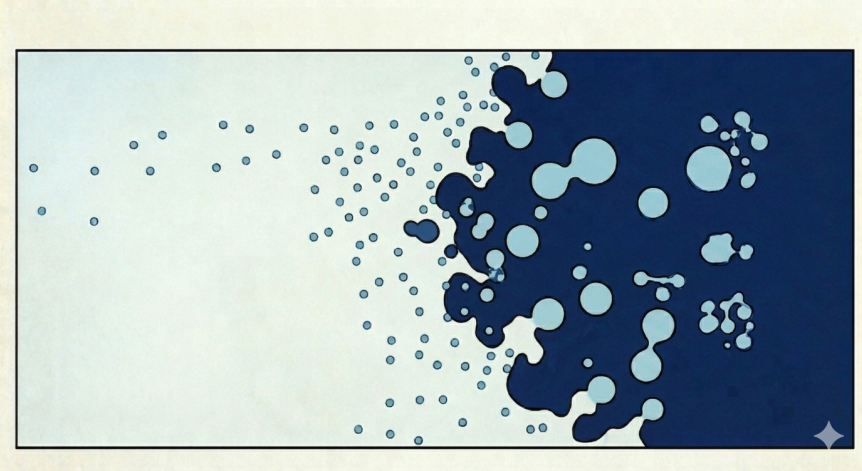

Sketch generated by Gemini

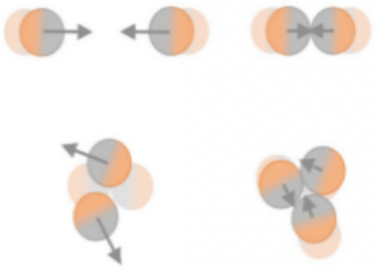

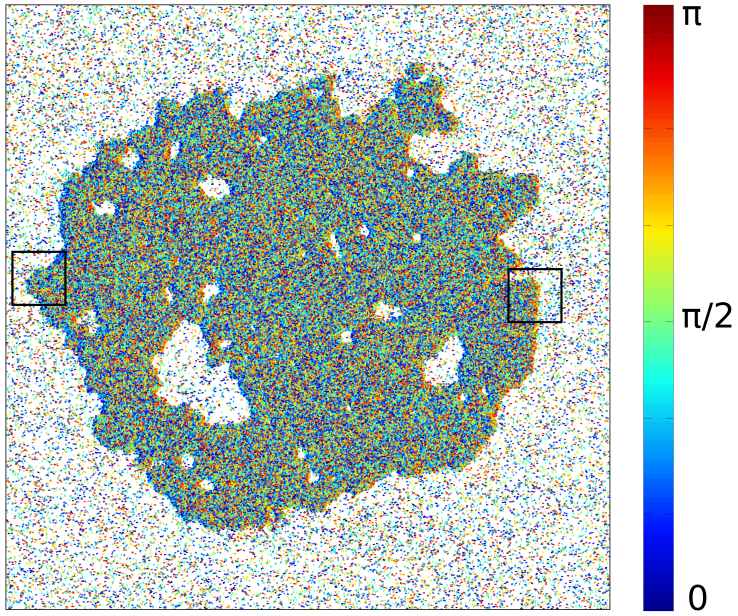

Particles collide heads on and aggregate even under repulsive interactions

Voronoi tessellation

Observable

A Voronoi diagram is induced by a set of points, called sites, that in our case are the centres of the disks.

The plane is subdivided into faces that correspond to the regions where one site is closest.

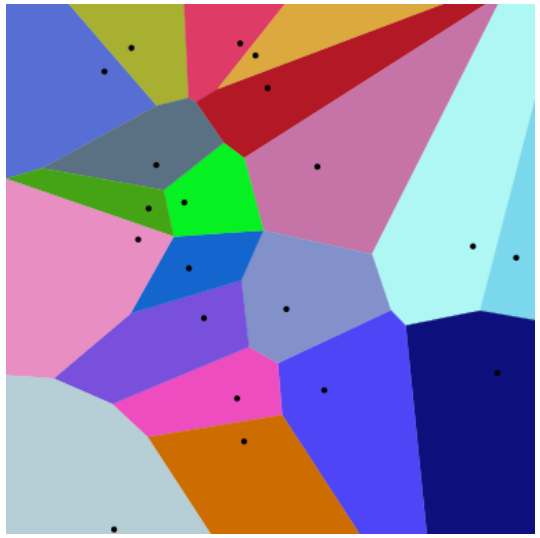

Focus on the central light-green face

All points within this region are closer to the dot within it than to any other dot on the plane

The region has five neighbouring cells from which it is separated by an edge

The grey zone has six neighbouring cells

Local density

Observable

For each bead, i, the first estimate of the local density ϕ_i^{Vor} is the ratio between its surface and the area A_i^{Vor} of its Voronoi region:

$$\phi_i^{\mathrm{Vor}} = \frac{\pi \sigma_{\mathrm{d}}^2}{A_i^{\mathrm{Vor}}}$$

We next coarse-grain this value by averaging the single-bead densities ϕ_i^{Vor} over a disk $S_\ell^{(i)}$ with radius ℓ

$$[[\phi_i]] \equiv \sum_{i \in S_\ell^{(i)}} \phi_i^{\mathrm{Vor}} / (\pi \ell^2)$$

MIPS

Identification via the local density distributions - dense & gas

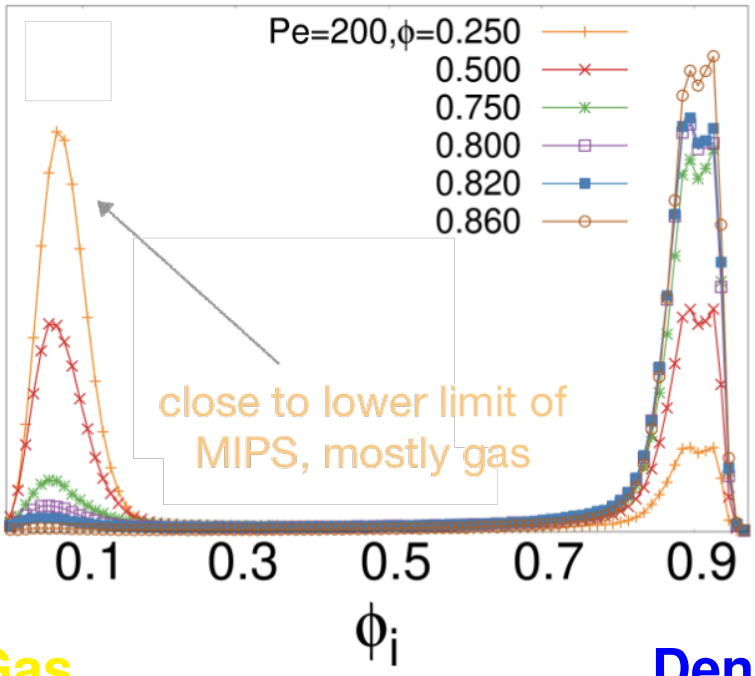

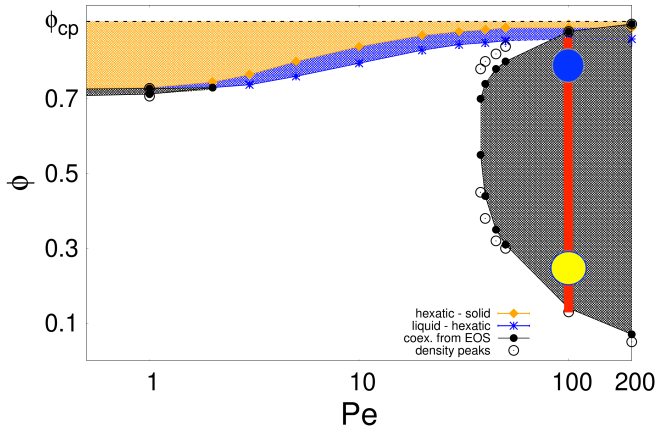

Gas **Dense**

The position of the peaks does not change while changing the global packing fraction ϕ but their relative height does. Transfer of mass from **gas** to **dense** component as ϕ increases

The Dense Phase

Hexatic patches, defects & bubbles in the stationary limit

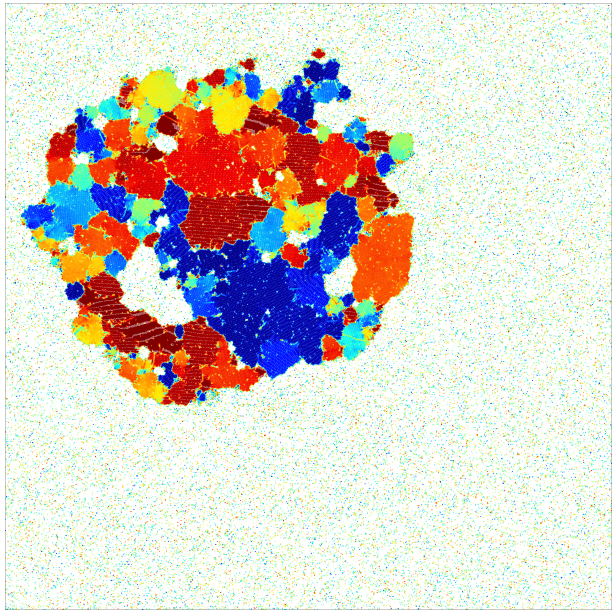

Dense/dilute separation[1]

For low packing fraction ϕ

a single round droplet

Growth[2] of clusters[3] with a mosaic

of hexatic orders[3] with

gas bubbles[2,4,5] & defects[6]

[1] Cates & Tailleur, Annu. Rev. Cond. Matt. Phys. 6, 219 (2015)

[2] Caporusso, Digregorio, Levis, LFC & Gonnella, PRL 125, 178004 (2020)

[3] Caporusso, LFC, Digregorio, Gonnella, Levis & Suma, PRL 131, 068201 (2023)

[4] Tjhung, Nardini & Cates, PRX 8, 031080 (2018)

[5] Shi, Fausti, Chaté, Nardini & Solon, PRL 125, 168001 (2020)

[6] Digregorio, Levis, LFC, Gonnella & Pagonabarraga, Soft Matter 18, 566 (2022)

The Coloured Patches

Local hexatic order parameter video

Orientational order

Local hexatic order parameter

$$\psi_{6j} = \frac{1}{N_{\rm nn}^{(j)}} \sum_{k=1}^{N_{\rm nn}^{(j)}} e^{{\rm i}6\theta_{jk}}$$

$N_{\rm nn}^{(j)}$ nearest-neighbours of the Voronoi cell

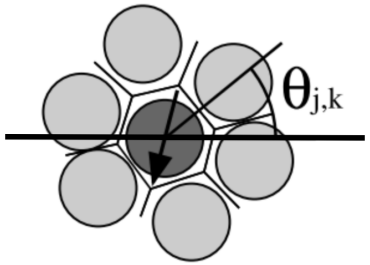

video

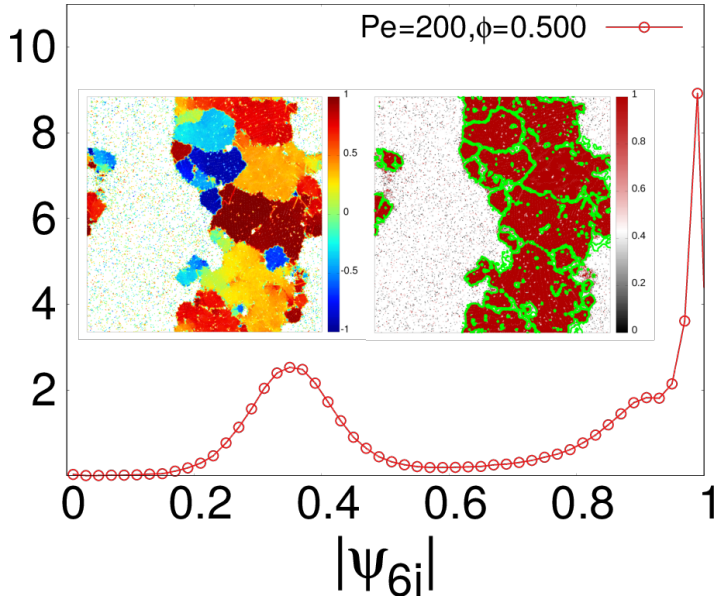

gas dense

in correspondence with the peaks of the distribution of local densities

$$P(R_H) \sim e^{-R_H/R_H^*}$$

Interfaces

Macro vs micro

Stationary state - video

Local hexatic order map Local density map

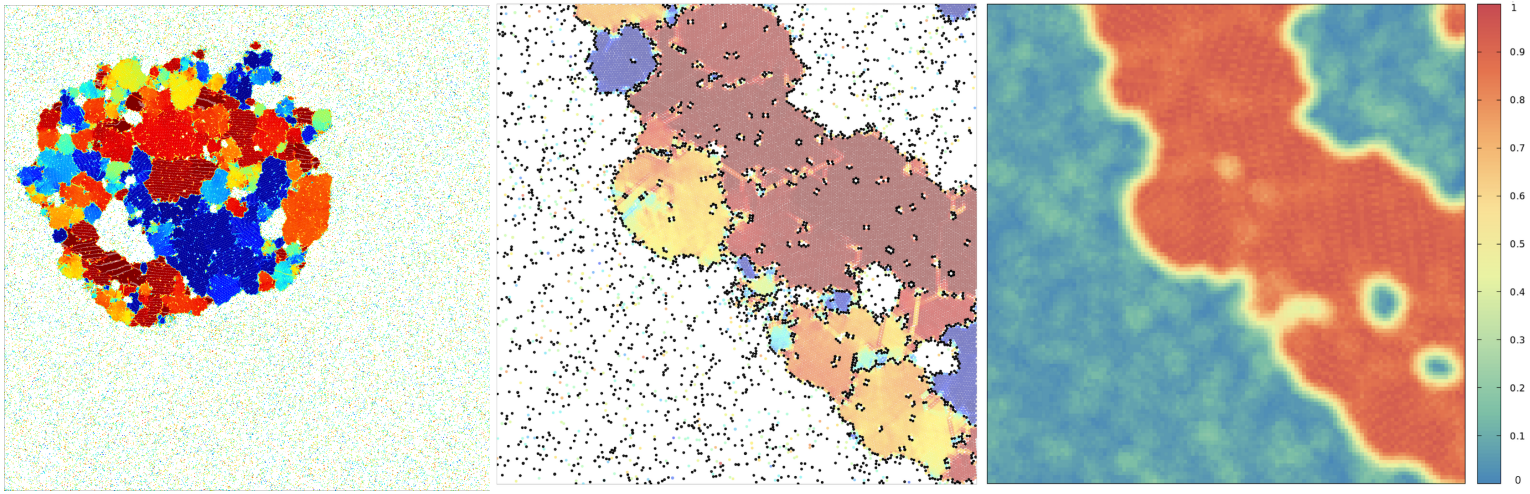

Local hexatic order saturates to a system size independent value

Defects on the boundaries between different hexatic ordered patches

Bubbles within the dense droplet

Interfaces

Strings of defects – along hexatic-hexatic interfaces

Hexatic order map

Defects

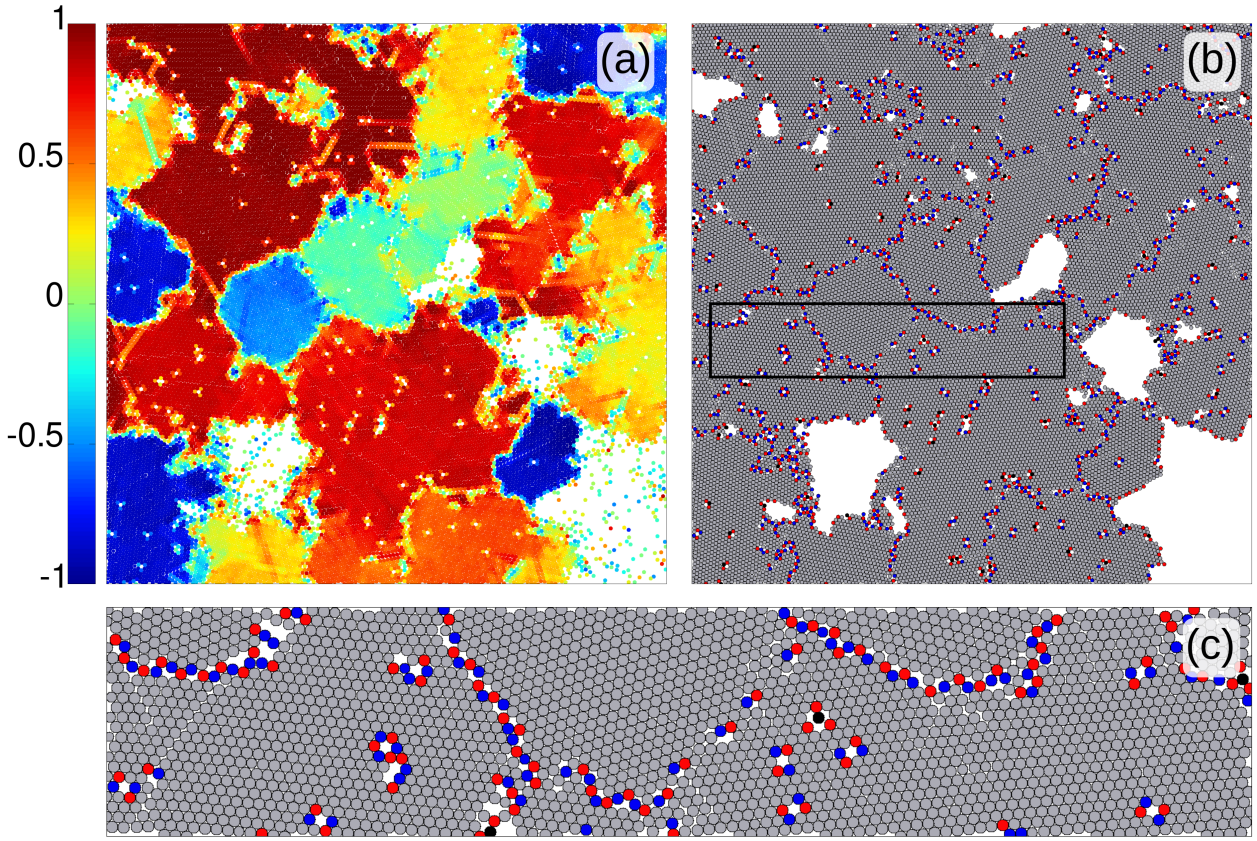

Zoom over the rectangular selection. Disks with **five** & **seven** neighbours

Clusters of defects

Size distribution - Finite size cut-off

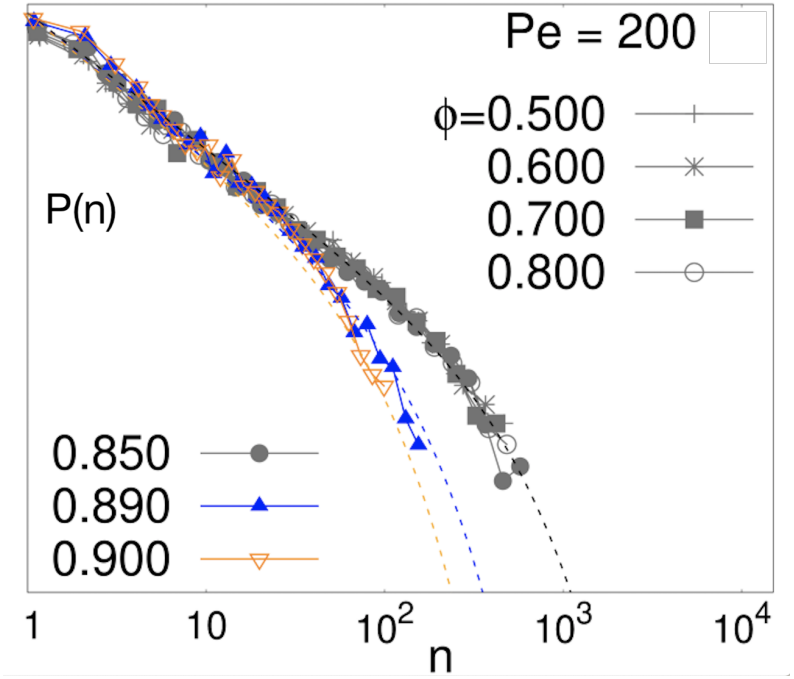

$$P(n) \simeq n^{-\tau} e^{-n/n^*}$$

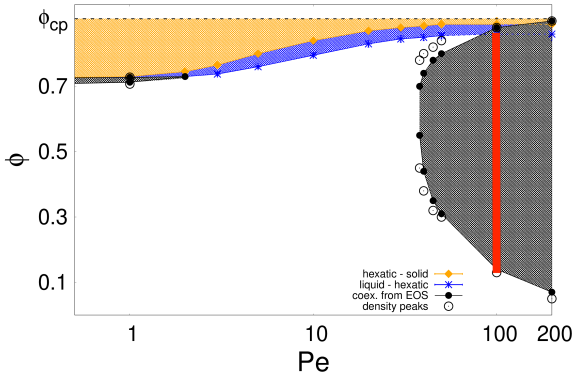

Independence of ϕ at fixed Pe within MIPS

$n^* \sim 30, 50, 200$ in the **solid**, **hexatic** and **MIPS**, respectively, and $\tau \sim 2.2$

No percolation, interrupted by the bubbles

Bubbles in Cavitation

At the interfaces between coloured patches bubbles pop up

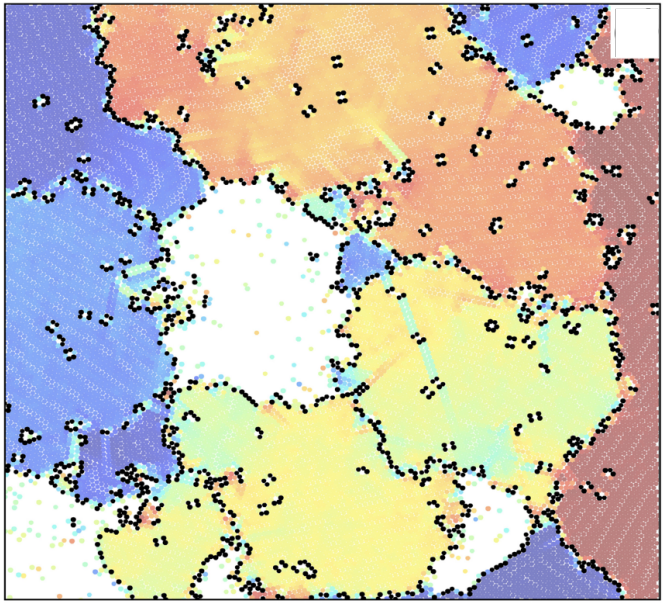

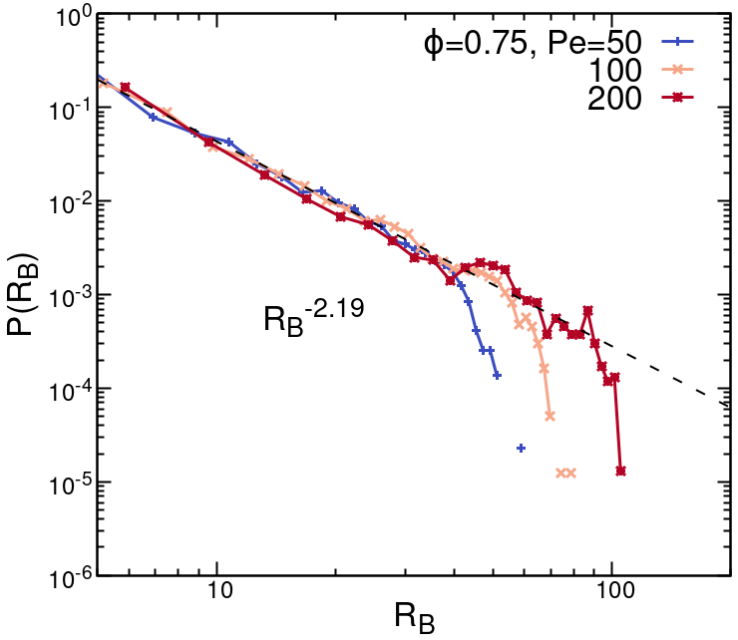

Bubbles appear and disappear at the interfaces between hexatic patches

Algebraic distribution of bubble sizes with a Pe-dependent exponential cut-off

Active Brownian Matter

Table with results

	Disks	Dumbbells
Non-eq Steady-State	$R \sim aL$ $R_H \sim R_H^* \ll L$ $P(R_B) \sim R_B^{-\tau} e^{-\frac{R_B}{R_B^*}}$	
Approach to NESS	**Next**	

Dynamics of phase separation

Phase separation

Mechanisms and laws

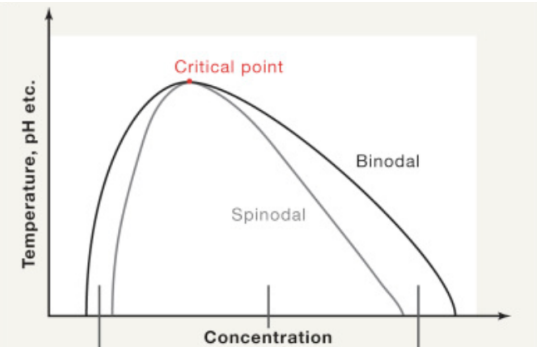

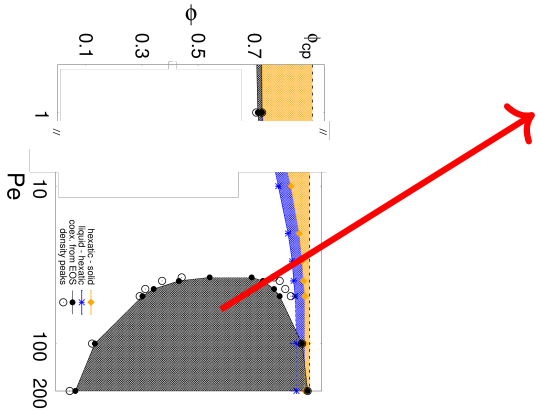

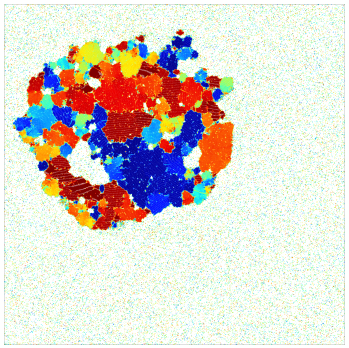

Dynamics of formation of the dense phase ? bubbles, hexatic order, ...

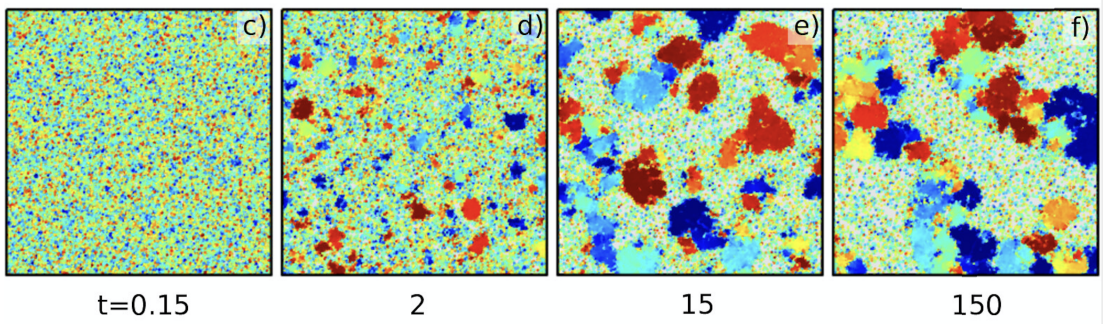

Universality with the Lifshitz-Slyozov law $R(t) \simeq t^{1/3}$? Geometry ?

Redner *et al* **13, Stenhammar** *et al* **14, ... , Caporusso** *et al* **20, Caprini** *et al* **20, ...**

The Growth Law

Growing length of the dense component and regimes

Different Pe

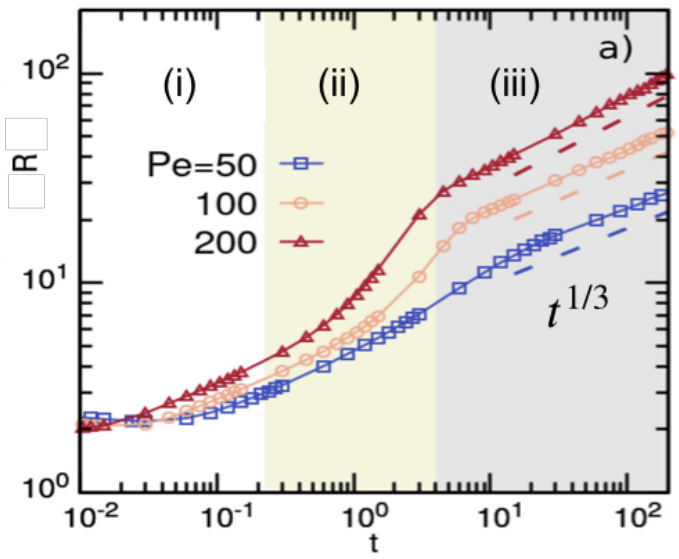

(i) nucleation (ii) condensation (iii) scaling

Movie

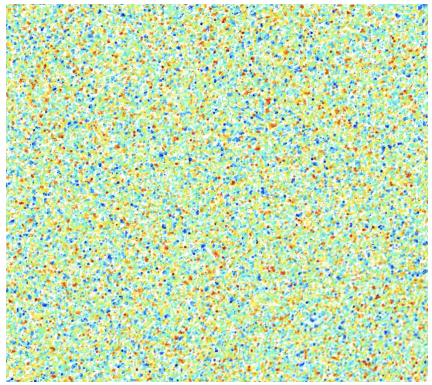

$R(t) \sim t^{1/3}$ for all Pe

Lifshitz-Slyozov-Wagner

In scaling regime $t^{1/3}$ like in passive scalar phase separation.

Redner *et al* **13, Stenhammar** *et al* **14, ... , Caporusso** *et al* **20, Caprini** *et al* **20, ...**

The growth law

Scaling of the structure factor

Different Pe

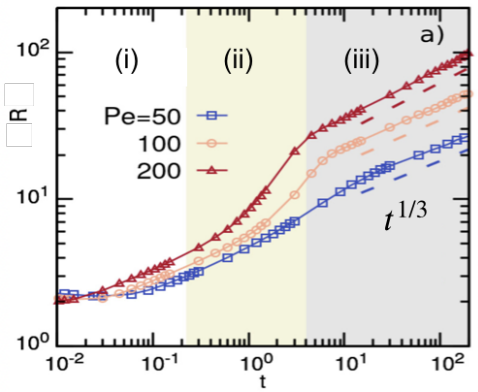

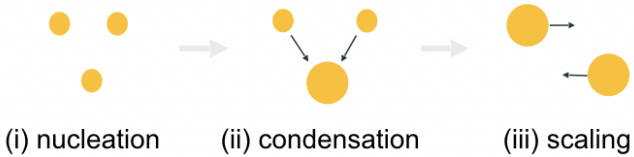

scaling

I peak: system average size

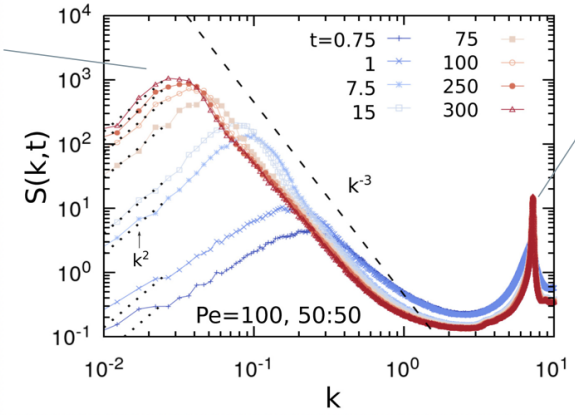

II peak: particles' packing

$$S(\mathbf{k},t) = \sum_{i=1}^{N} e^{i\mathbf{k}(\mathbf{r}_i - \mathbf{r}_j)}$$

related to Fourier transform of the pair correlation function

$$S(k,t) \sim R(t)^d \, f(kR(t))$$

Dynamic

In **scaling regime** $t^{1/3}$ like in **Lifshitz-Slyozov-Wagner**, scalar phase separation

Lifshitz & Slyozov 61, Wagner 61, Huse 93, Bray 94 review

Hexatic structure factor

Growing length of hexatic order

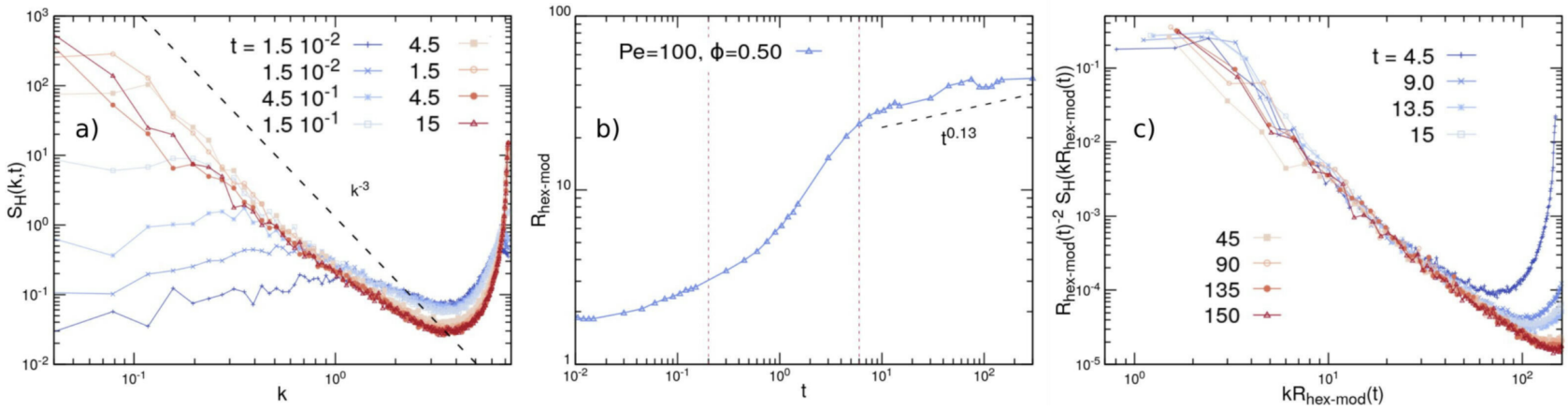

Hexatic Structure factor

$$S_H(\boldsymbol{q}) = \langle |\psi_{6j}|(\boldsymbol{q})|\psi_{6j}|(-q)\rangle$$

Growing hexatic length

$$R_H \sim t^{0.13}$$

Scaling

$$kR_H(t)$$

Local Hexatic Order

Growing length of the orientational order

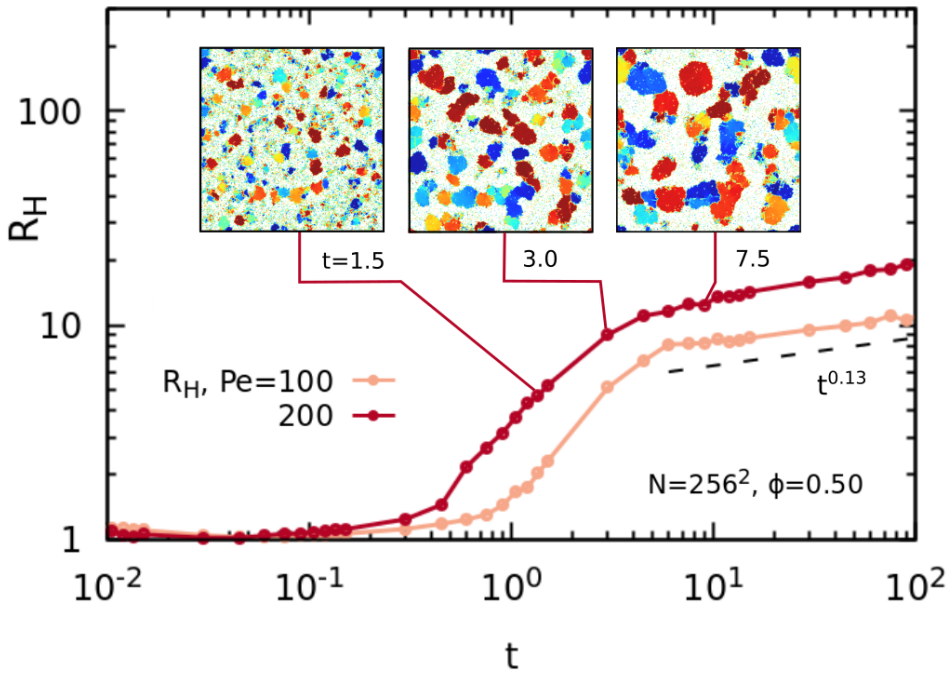

Full hexatically ordered small clusters

Local hexatic order parameter

$$\psi_{6j} = \frac{1}{N_{\rm nn}^{(j)}} \sum_{k=1}^{N_{\rm nn}^{(j)}} e^{{\rm i}6\theta_{jk}}$$

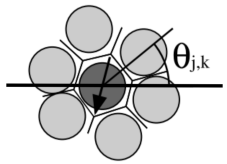

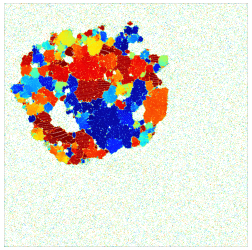

Larger clusters with several orientational order within

$R_H \sim t^{0.13}$ in the scaling regime and $R_H \to R_H^* \ll L$

Similar to pattern formation, e.g.

Vega, Harrison, Angelescu, Trawick, Huse, Chaikin & Register 05

Macro vs. Micro - ABP

Dense phase vs. hexatic growth

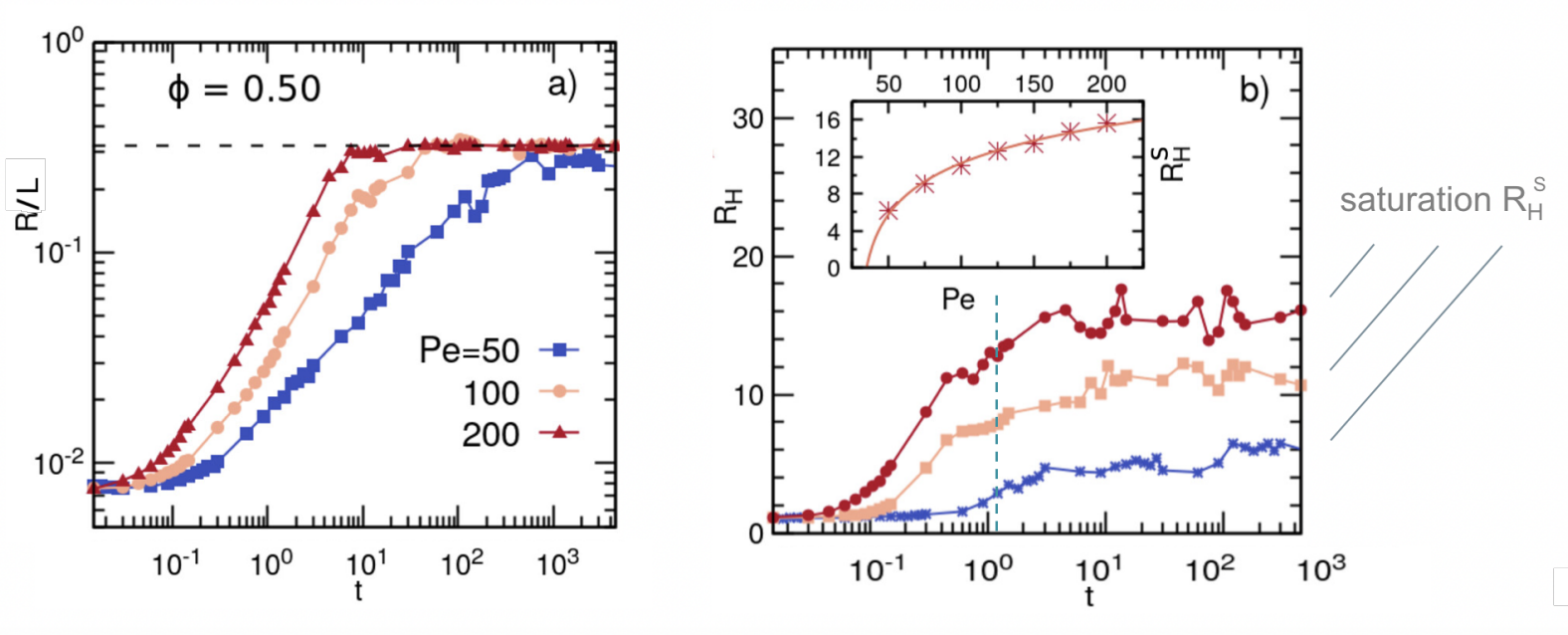

$R(t) \to aL$

$R_H(t) \to R_H^*$ finite $\quad R_H^* \nearrow$ Pe $\nearrow$

Active Brownian Matter

Table with results

	Disks	Dumbbells
Non-eq Steady-State	$R \sim aL$ $R_H \sim R_H^* \ll L$ $P(R_B) \sim R_B^{-\tau} e^{-\frac{R_B}{R_B^*}}$	
Approach to NESS	$R \sim t^{1/3} \to aL$ $R_H \sim t^{0.13} \to R_H^*$	

Mechanism for $t^{1/3}$

Two (non-exclusive) possibilities

1. Is it like the one of **passive attractive particles** ?

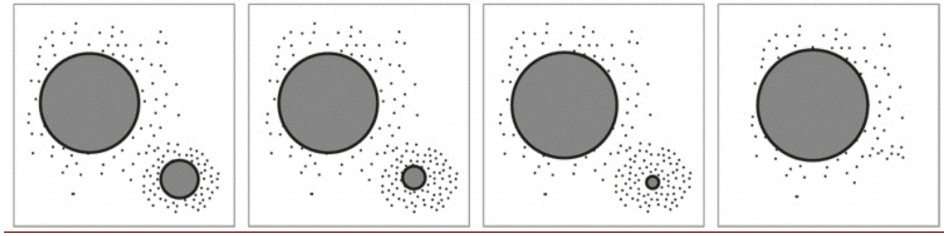

Ostwald ripening

2. Are there other **processes** at work in the active case ?

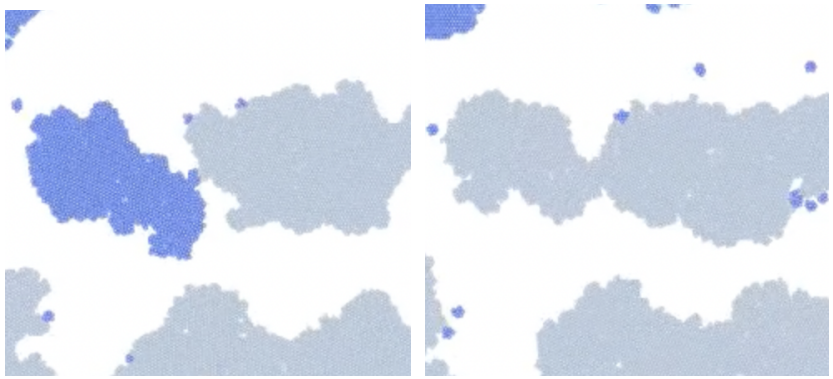

Cluster-cluster aggregation

Focus on Clusters

Dense Clusters

Instantaneous configurations (DBSCAN)

Passive - attractive

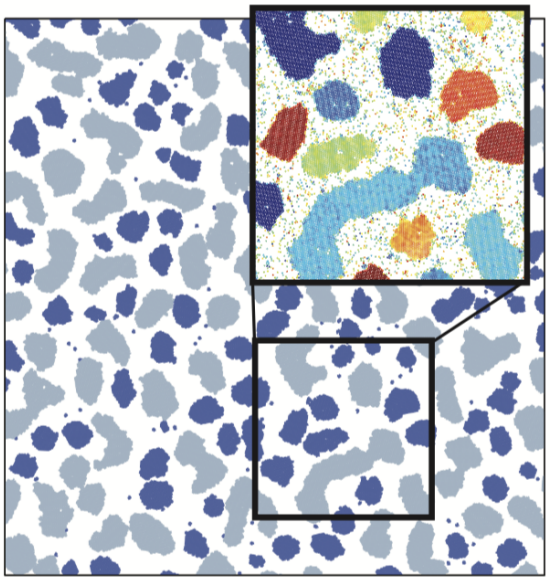

Active - repulsive

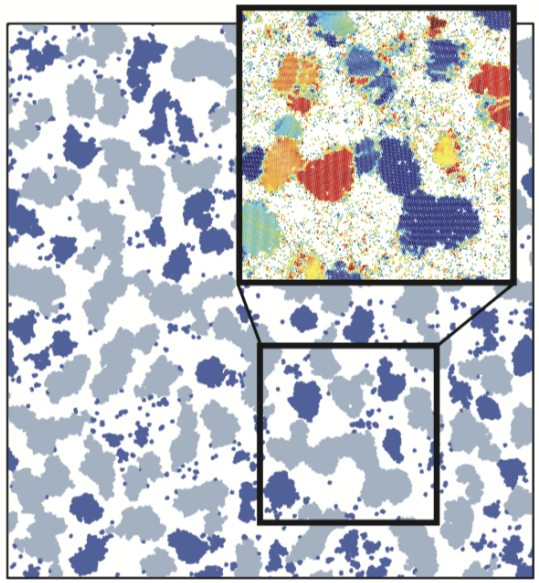

The Mie potential is not truncated in the passive case $\Rightarrow$ attractive

Parameters are such that $R(t)$ is the same in the two systems

Colors in the zoomed box indicate orientational order

Caporusso, LFC, Digregorio, Gonnella, Levis & Suma 23

Geometry

Scatter plots: small regular – large fractal

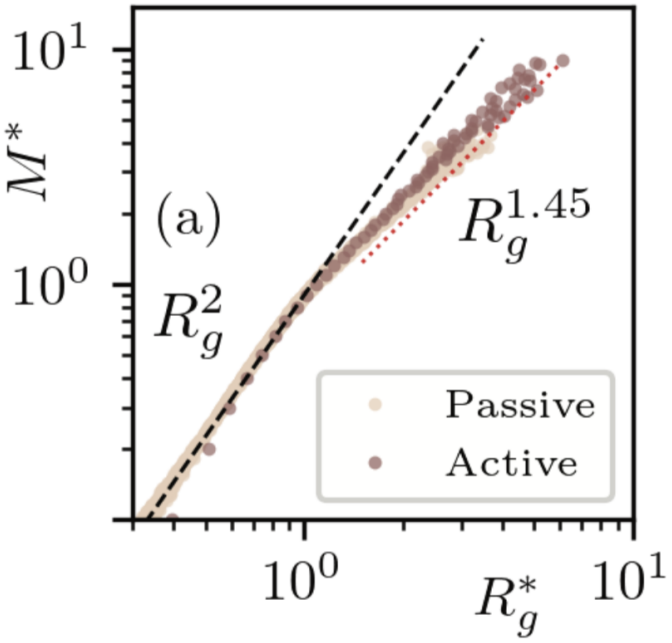

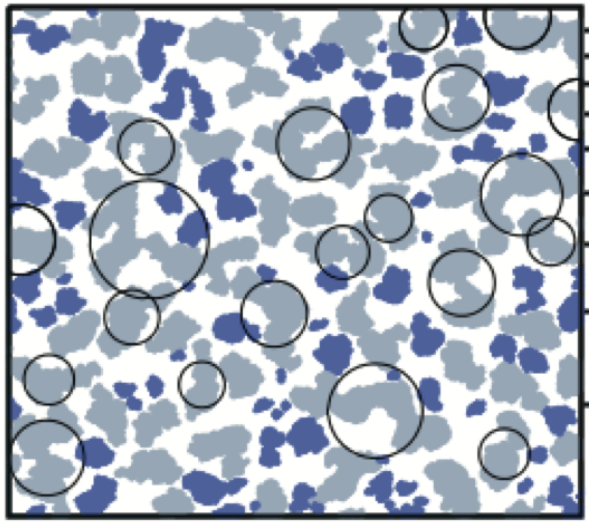

Cluster mass $M^*(t) = \dfrac{M_k(t)}{\overline{M}(t)}$ Gyration radius $R_g^*(t) = \dfrac{R_{g_k}(t)}{\overline{R_g}(t)}$

Data sampled in the scaling regime $t = 10^3 - 10^5$ every 10^3 time steps

$\overline{M}(t) = \dfrac{1}{N_c(t)} \sum_{k=1}^{N_c(t)} M_k(t)$ and $N_c(t)$ the total number of clusters at time t

Clusters' Dynamics

Tracking of individual cluster motion - video

Active

Passive

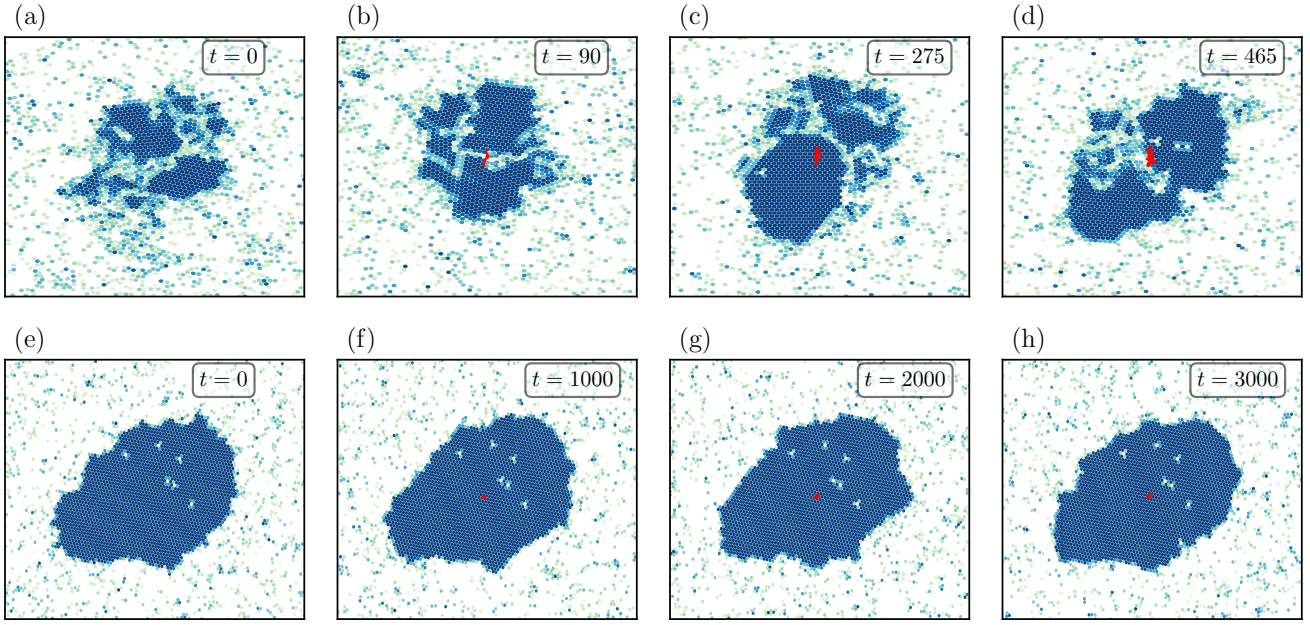

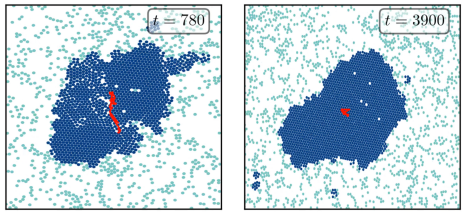

In **red** the center of mass trajectory

Active is much faster than passive

Dense Clusters

Visual facts about the instantaneous configurations

Similarities

- Large variety of shapes and sizes (masses)

  Co-existence of

  small regular (**dark blue**) and large elongated (**gray**) clusters

Differences

- Rougher interfaces in active
- Homogeneous (passive) vs. heterogeneous (active) orientational order within the clusters

Dense Clusters

Visual facts about their dynamics

In both cases, **Ostwald ripening** features

- small clusters evaporate
- gas particles attach to large clusters

In the **active system**

- clusters displace much more & sometimes aggregate
- they also break & recombine

like in **diffusion limited cluster-cluster aggregation**

Clusters' Diffusion

Mean Square Displacement

Average over all clusters

Mass dependence

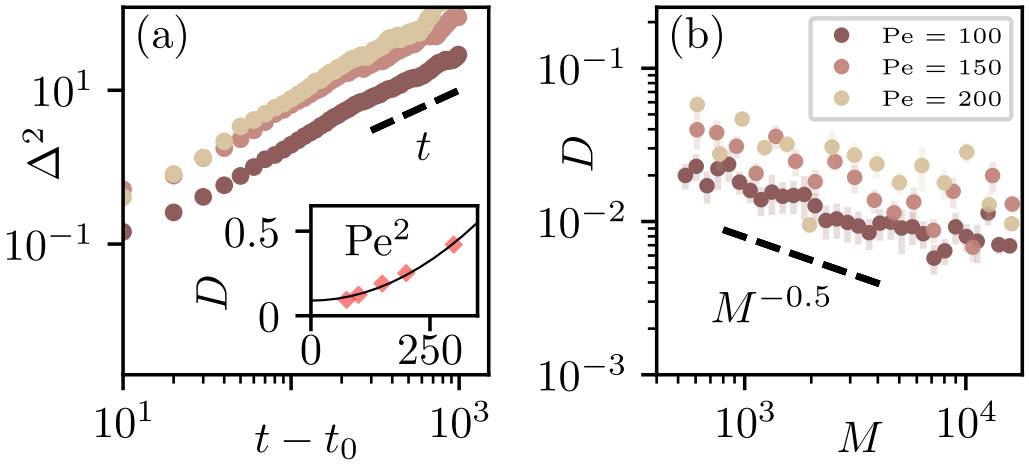

$$D \sim M^{-1/2}$$

$$\Delta_k^2(t, t_0) = [\mathbf{r}_{\mathrm{c.o.m.}}^{(k)}(t) - \mathbf{r}_{\mathrm{c.o.m.}}^{(k)}(t_0)]^2 \sim 2d\, D(M_k, \mathrm{Pe})\,(t - t_0)$$

A sum of random forces yields $D \sim M^{-1}$

Passive tracer in a dilute active bath $D \sim R^{-1} \sim M^{-1/2}$ **Solon & Horowitz 22**

Passive & very heavy isolated active clusters $D \sim M^{-1}$

Cluster-Cluster Aggregation

Smoluchowski argument

From $\overline{R}_g \sim t^{1/z}$ and using $D(M) \sim M^{-\alpha}$

Smoluchowski eq. $\Rightarrow z = d_f(1+\alpha) - (d - d_w)$

Regular clusters $M_k < \overline{M}$

$d_f = d = d_w = 2$

$\alpha = 0.5$

$z = 2(1 + 0.5) = 3$

Fractal clusters $M_k > \overline{M}$

$d_f = 1.45, d = 2$ and $d_w \sim 2$

$\alpha = 0.5$ in the bulk

$z = 1.45(1 + 0.5) = 2.18 < 3$

Reviews on the application of fractals to colloidal aggregation

Jullien 92 Meakin 92

Active Brownian Matter

Table with results

	Disks	Dumbbells
Non-eq Steady-State	$R \sim aL$ $R_H \sim R_H^* \ll L$ $P(R_B) \sim R_B^{-\tau} e^{-\frac{R_B}{R_B^*}}$	**Next**
Approach to NESS	$R \sim t^{1/3}$ $R_H \sim t^{0.13}$ Ostwald ripening & Cluster-cluster aggregation Thanks to $D(M) \sim M^{-1/2}$	**Next**

Active Brownian Dumbbells

e.g., a diatomic molecule or a dumbbell

Two spherical atoms with diameter σ and mass m

Massless spring modelled by a finite extensible non-linear elastic (fene) force between the atoms $\mathbf{f}_{\text{fene}} = -\dfrac{k(\mathbf{r}_i - \mathbf{r}_j)}{1 - r_{ij}^2/r_0^2}$ with an additional repulsive contribution (WCA potential) to avoid atomic/colloidal overlapping (see next slides)

Langevin modelling of the interaction with the embedding fluid:

isotropic viscous forces, $-\gamma\dot{\mathbf{r}}_i$, and independent noises, $\boldsymbol{\xi}_i$, on the beads.

Translational motion (centre of mass)

Rotations due to effective torque applied by noise

Vibrations due to the fene potential (frozen)

Phase Diagram

Plenty of differences induced by the particle shape

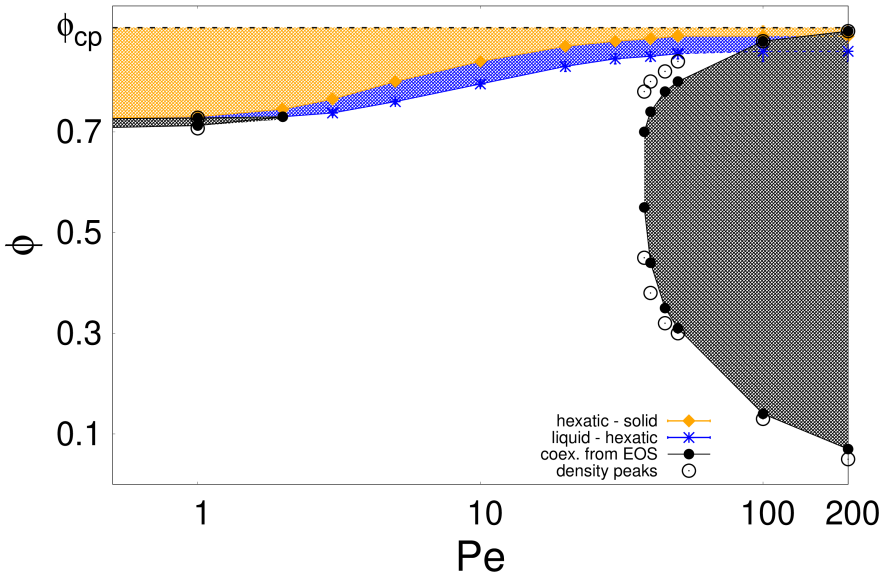

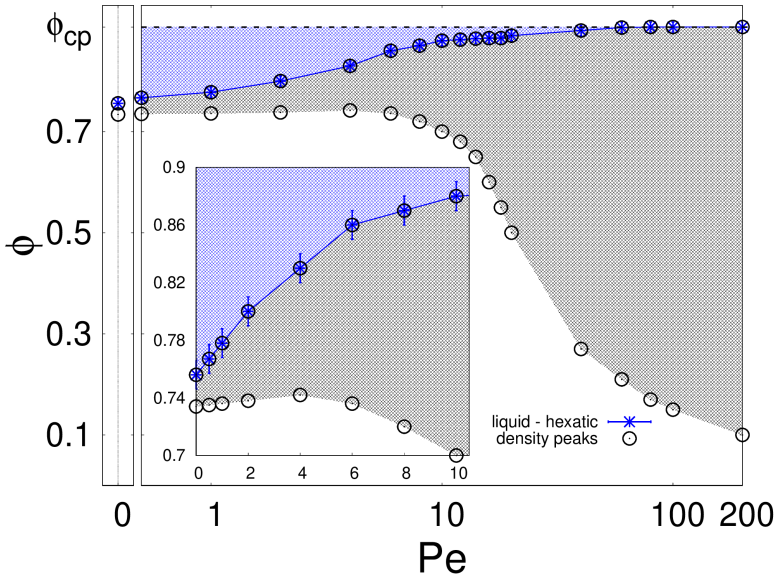

AB Disks

AB Dumbbells

LFC, Digregorio, Gonnella & Suma 17

Growth of the Dense Phase

Disks vs Dumbbells both at Pe = 100 and 50 : 50

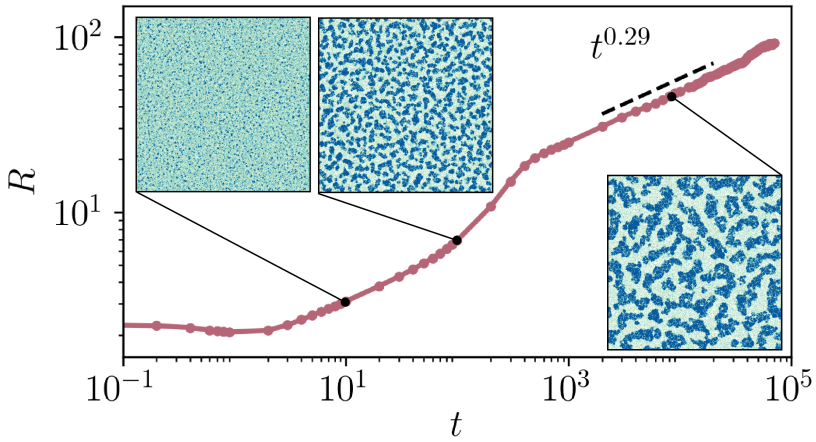

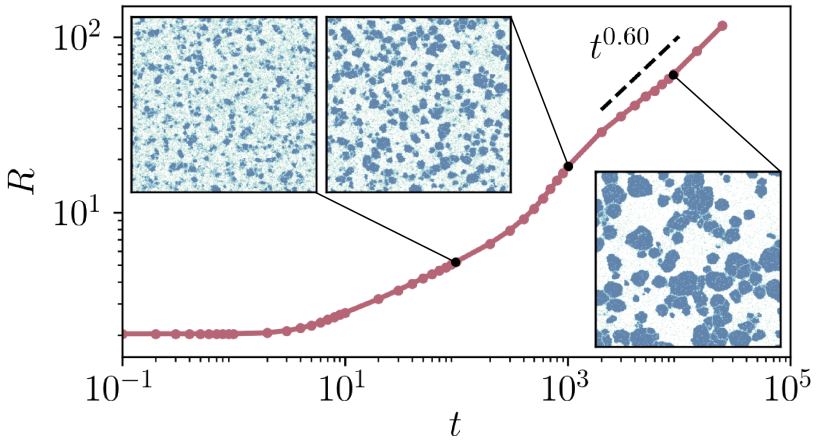

AB Disks

slower

$t^{0.3}$

AB Dumbbells

faster

$t^{0.6}$

Caporusso, LFC, Digregorio, Gonnella & Suma 24

Local Hexatic Order - ABD

Growth towards saturation

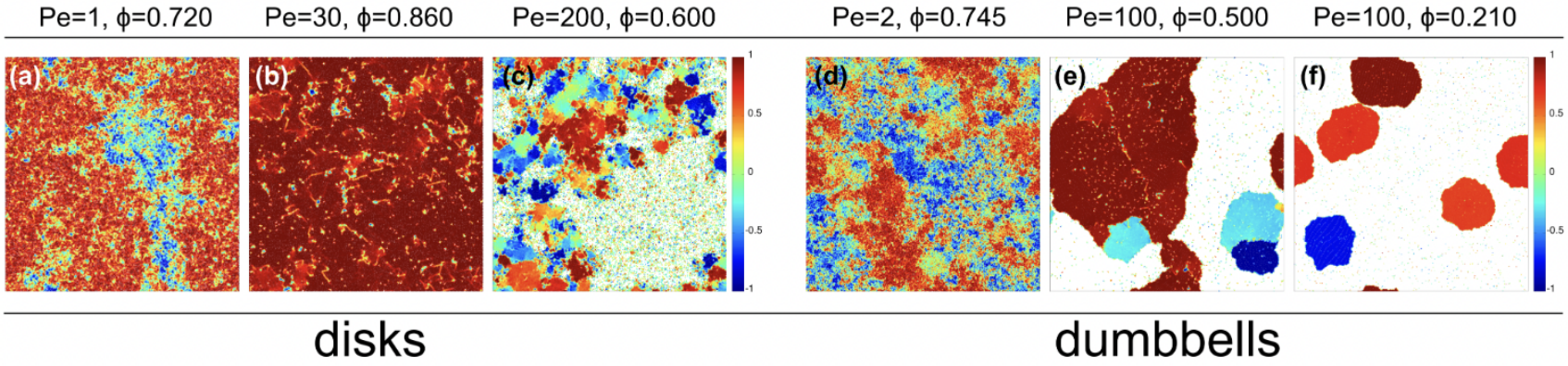

Video

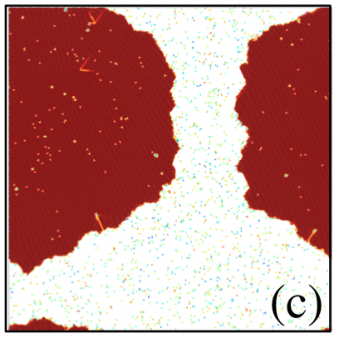

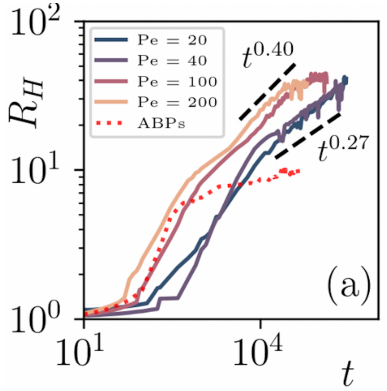

$$R_H \sim t^{0.3} \to R$$

Faster growth than for ABPs, full orientational order is reached & no bubbles

Caporusso, LFC, Digregorio, Gonnella & Suma 24

Isolated Dumbbell Clusters

Motion

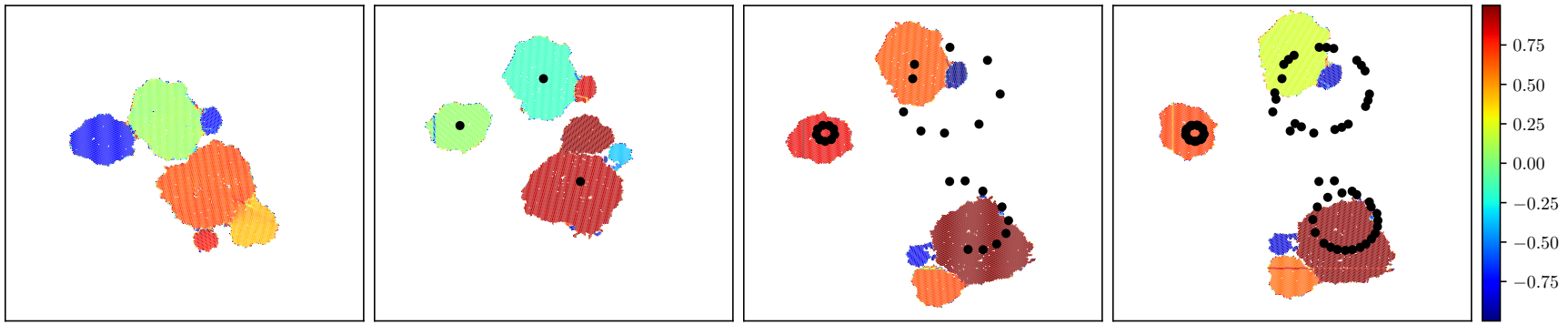

time

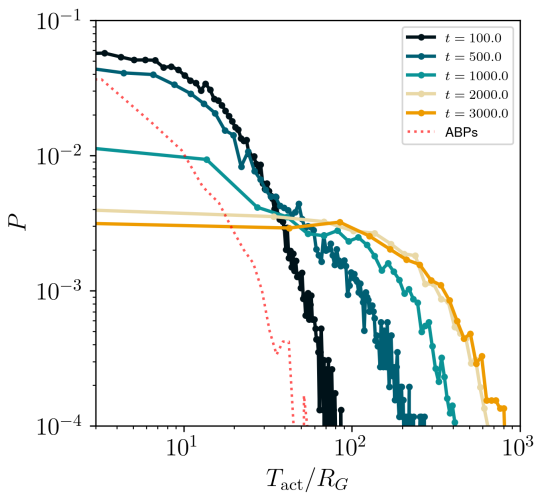

- Instability of clusters with multi-orientational order : they break up along the hexatic interfaces
- The center of mass (c.o.m.) of each cluster α rotates with constant angular velocity ω_α
- The clusters rotate around their c.o.m. with the same angular velocity ω_α

Torque

Solid body motion

Active Brownian Matter

Table with results

	Disks	Dumbbells
Non-eq Steady-State	$R \sim L$ $R_H \sim R_H^* \ll L$ $P(R_B) \sim R_B^{-\tau} e^{-\frac{R_B}{R_B^*}}$	$R \sim L$ $R_H \sim L$ no bubbles
Approach to NESS	$R \sim t^{1/3} \to L$ $R_H \sim t^{0.13} \to R_H^*$ Ostwald ripening & Cluster-cluster aggregation	$R \sim t^{2/3} \to L$ $R_H \sim t^{0.3} \to L$ Rotation polarization

Disks vs. Dumbbells

What is special about dumbbells ?

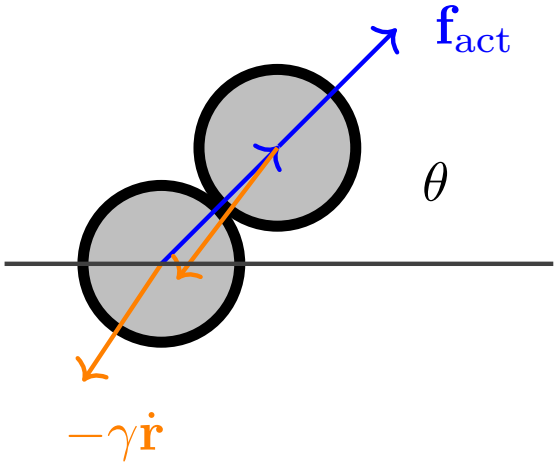

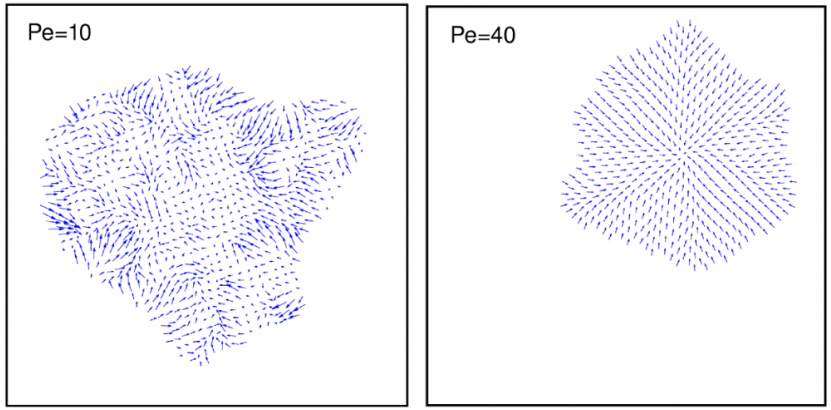

Coarse-grained **polarization**

Vortex & aster patterns emerge

Petrelli, LFC, Digregorio, Gonnella & Suma 18

Disks vs Dumbbells

Field Theory - density ϕ coupled to polarity p

$$F = \int d^d x \left\{ \frac{\alpha_\phi}{2\phi_{cr}} \phi^2 (\phi - \phi_0)^2 + k_\phi |\nabla \phi|^2 - \alpha_{\boldsymbol{p}} \frac{\phi - \phi_{cr}}{\phi_{cr}} |\boldsymbol{p}|^2 + \frac{\alpha_{\boldsymbol{p}}}{2} |\boldsymbol{p}|^4 + k_{\boldsymbol{p}} (\nabla \boldsymbol{p})^2 \right\}$$

$$\partial_t \phi + \boxed{\lambda \nabla \cdot (\boldsymbol{p}\phi)} = M \nabla^2 \mu_\phi$$

$$\partial_t \boldsymbol{p} = -\Gamma \boldsymbol{\mu_p}$$

$$R(t) \simeq t^{0.6} \qquad \lambda = 10^{-2}$$

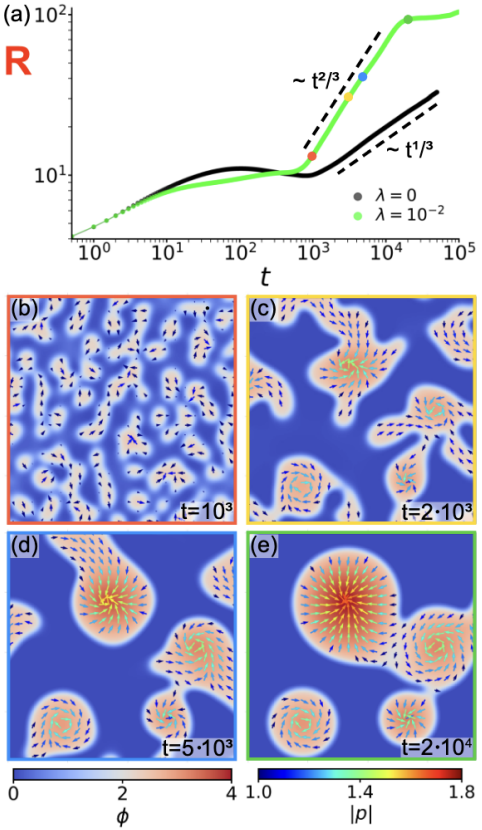

Advection accelerates growth

$$\mu_\phi = \frac{\delta F}{\delta \phi} \qquad \boldsymbol{\mu_p} = \frac{\delta F}{\delta \boldsymbol{p}}$$

$\lambda = 0$ Model B

Semeraro, LFC, Gonnella & Tiribocchi 25

Effective Temperature

Teff = T

Co-existence in equilibrium

Pe = 0 $\quad \phi = 0.710$

Integrated linear response & mean-square displacement: their ratio (FDT) $\tau = t - t_w$

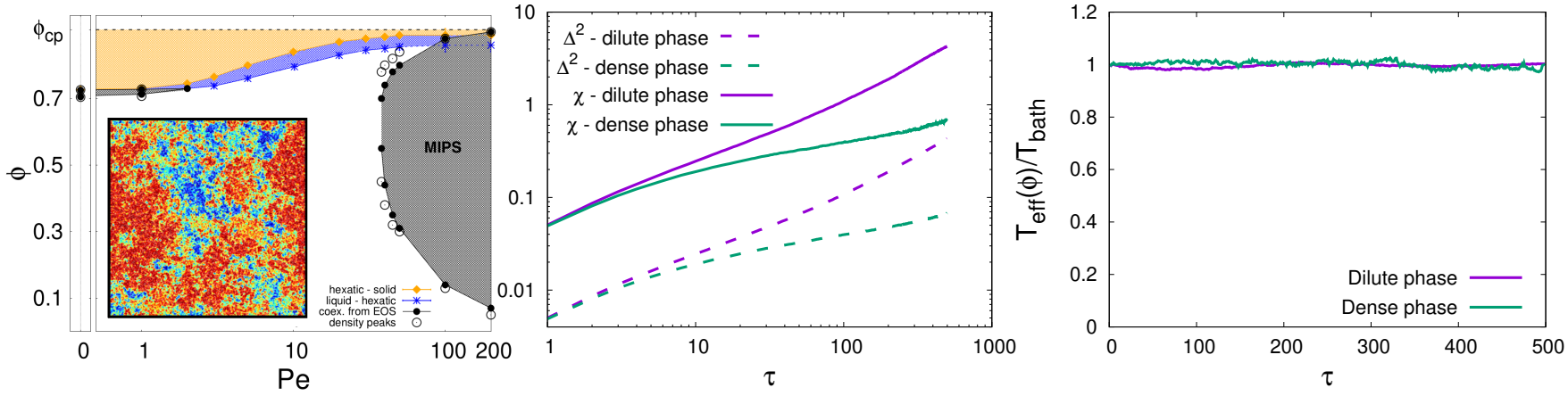

Method: linear response computed with Malliavin weights (no perturbation applied) as proposed by **Szamel** for active matter systems.

Petrelli, LFC, Gonnella & Suma 20

Teff $\neq$ T

Co-existence in MIPS

Pe = 50 $\quad \phi = 0.5$

Integrated linear response & mean-square displacement: their ratio (FDR) $\tau = t - t_w$

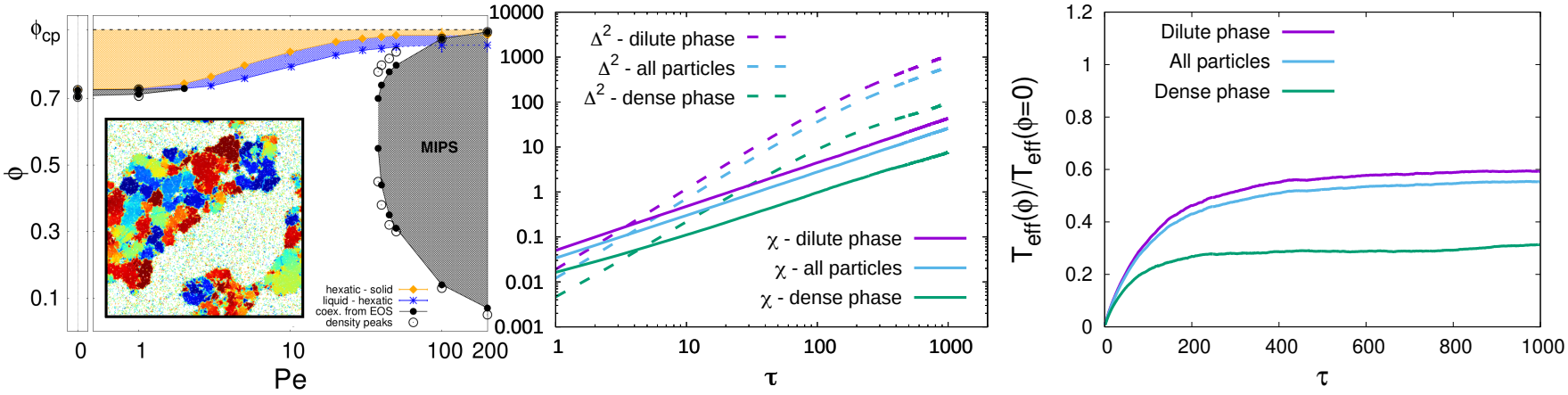

Method: linear response computed with Malliavin weights (no perturbation applied) as proposed by **Szamel** for active matter systems.

Petrelli, LFC, Gonnella & Suma 20

Teff in MIPS

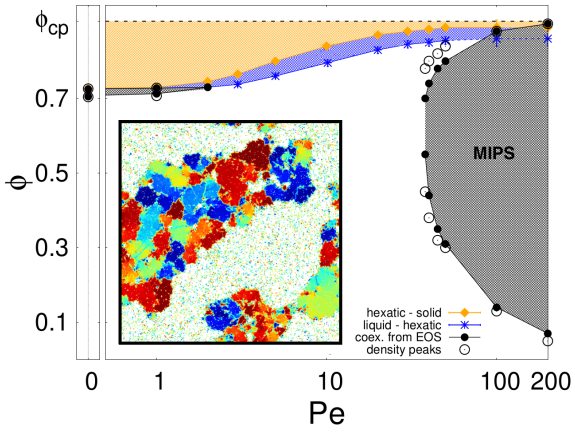
ϕ_{cp}
0.7
ϕ 0.5
0.3
0.1
0
1
10
100 200
Pe
MIPS
hexatic - solid
liquid - hexatic
coex. from EOS
density peaks

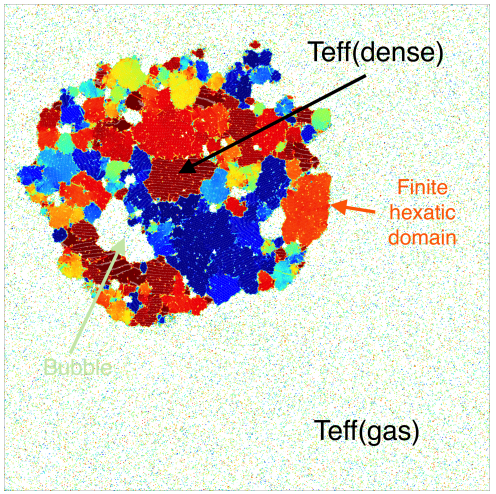
Teff(dense)
Finite hexatic domain
Bubble
Teff(gas)

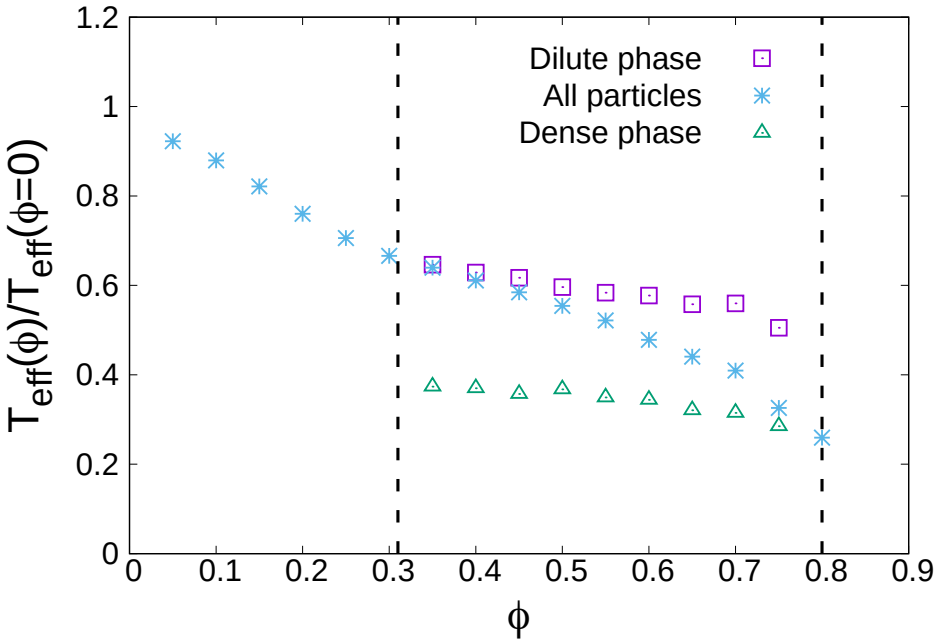
1.2
1
0.8
0.6
0.4
0.2
0
0
0.1
0.2
0.3
0.4
0.5
0.6
0.7
0.8
0.9
$T_{eff}(\phi)/T_{eff}(\phi=0)$
ϕ
Dilute phase
All particles
Dense phase

Results on disks & dumbbells

We established the full phase diagram of ABPs **solid**, **hexatic**, **liquid** & **MIPS**

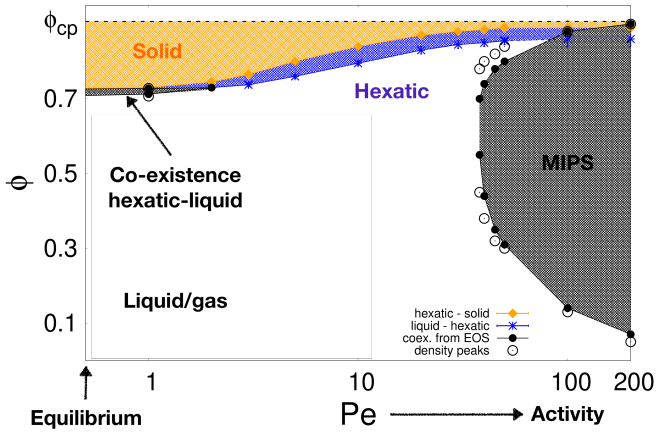

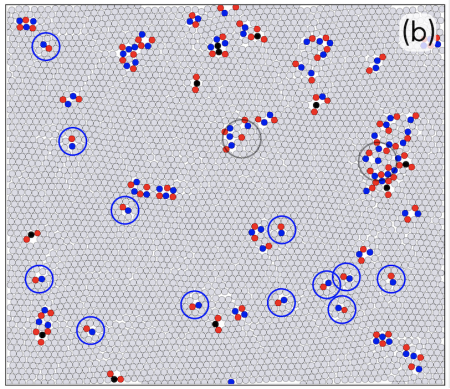

We clarified the role played by point-like (**dislocations** & **disclinations**) and **clustered** defects in passive & active $2d$ models.

In **MIPS**

Micro *vs.* macro: hexatic patches & bubbles

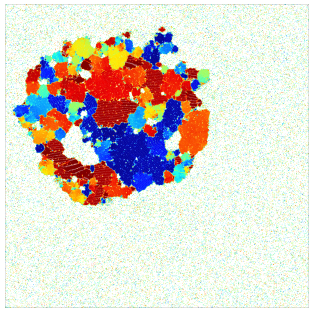

Results on disks & dumbbells

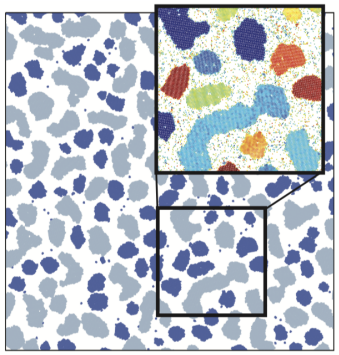

Difference between

Passive

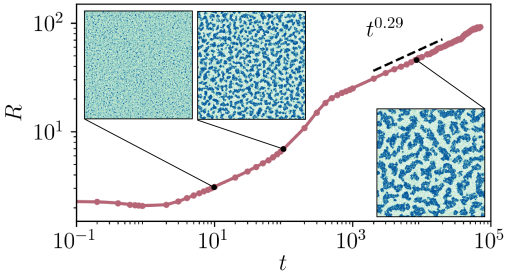

ABPs

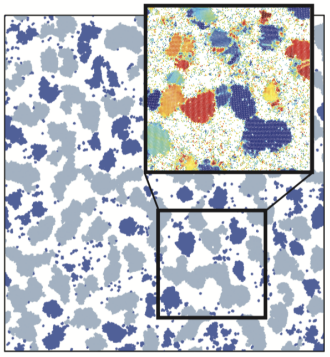

Active

growth

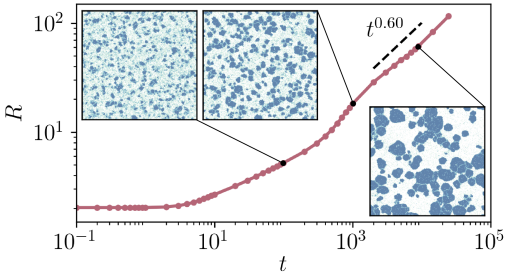

ABDs

Ostwald ripening & cluster-cluster diffusive aggregation in active case
cluster-cluster aggregation almost not present in passive

Co-existence of regular and fractal clusters

Heterogeneous orientational order in large active clusters

Plan

1. Classical Active Matter.
   - Real and artificial systems
   - Models
   - Phenomenology
2. **Quantum Active Matter**
   - Models
   - Phenomenology
   - Realizations ?
3. Perspectives

Quantum Active Particles

Sketches of three models - playing with the environments

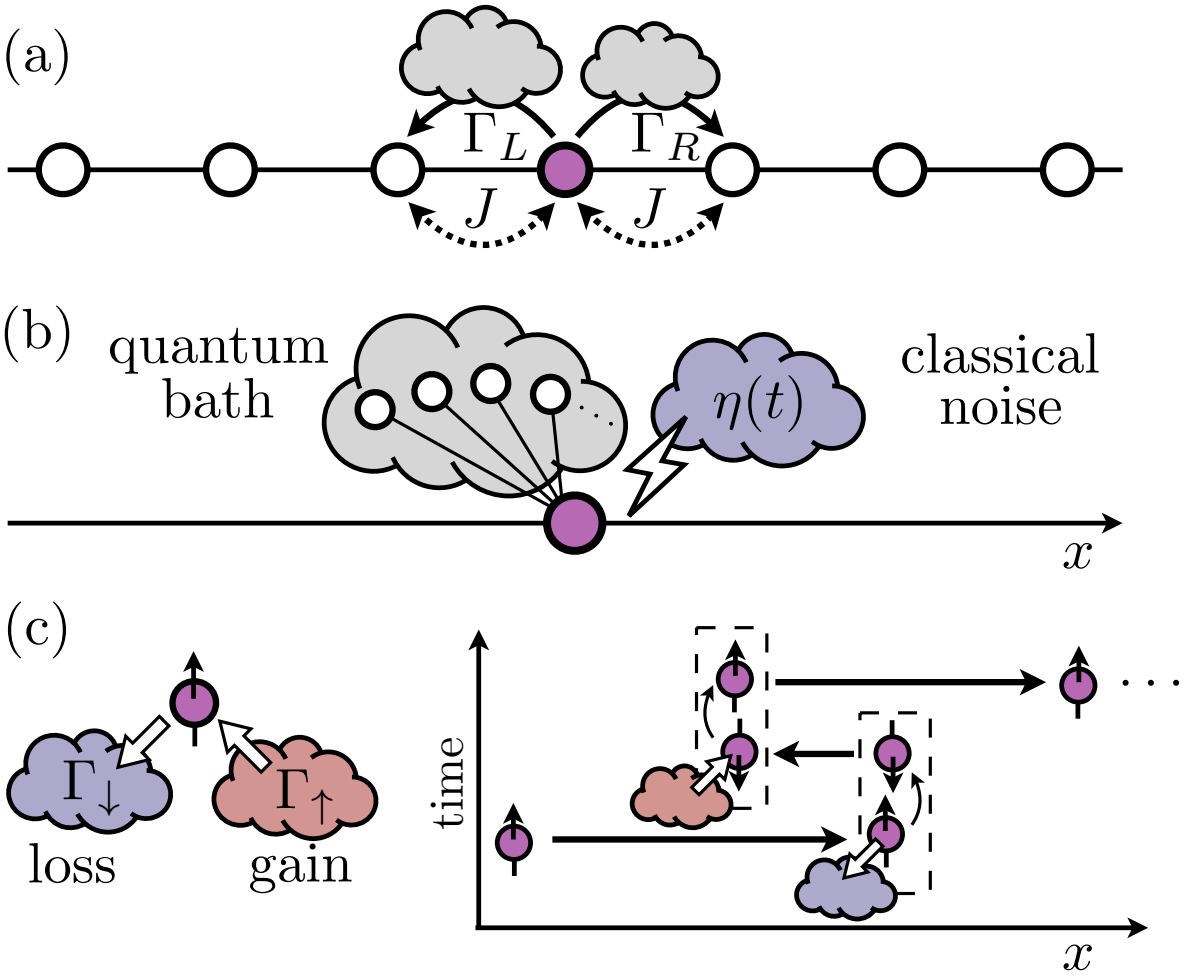

Quantum Active Particles

Purely quantum models (a) and (c)

Take a system with a time-independent Hamiltonian $\hat{\mathcal{H}}$

in a generic mixed state described by the density operator $\hat{\rho} = \sum_\alpha p_\alpha |\psi_\alpha\rangle\langle\psi_\alpha|$

with, e.g. $\{|\psi_\alpha\rangle\}$ a basis of Hilbert space & $\sum_\alpha p_\alpha = 1$

and in contact with an environment

The density operator ($\{p_\alpha\}$) depends on time and $\hat{\rho}$ obeys the **Lindblad eq**

$$\underbrace{\partial_t \hat{\rho} = -\frac{\mathrm{i}}{\hbar}[\hat{\mathcal{H}}, \hat{\rho}]}_{\text{Heisenberg}} + \underbrace{\sum_n \left(\hat{L}_n \hat{\rho} \hat{L}_n^\dagger - \frac{1}{2}\{\hat{L}_n^\dagger \hat{L}_n, \hat{\rho}\} \right)}_{\text{effect of the bath}}$$

where $\{\hat{L}_n\}$ are operators describing the effect of the environment

NB this eq is local in time - **no memory**

Choose $\hat{\mathcal{H}}$ and $\{\hat{L}_n\}$

Quantum Active Particles

Purely quantum models (a) and (c)

Take a system with a time-independent Hamiltonian $\hat{\mathcal{H}}$

in a generic mixed state described by the density operator $\hat{\rho} = \sum_\alpha p_\alpha |\psi_\alpha\rangle\langle\psi_\alpha|$

with, e.g., $\{|\psi_\alpha\rangle\}$ a basis of the Hilbert space & $\sum_\alpha p_\alpha = 1$

and in contact with an environment

The observables are calculated as, e.g.,

$$\mathrm{Var}(\hat{x}(t)) = \langle(\hat{x}(t) - \langle\hat{x}(t)\rangle)^2\rangle$$

with $\langle\hat{A}(t)\rangle = \mathrm{Tr}(\hat{A}\hat{\rho}(t))$

a bit like the Fokker-Planck description of the classical problems (no memory)

Choose $\hat{\mathcal{H}}$ and $\{\hat{L}_n\}$

Environment-assisted hopping

on a one dimensional lattice with periodic boundary conditions

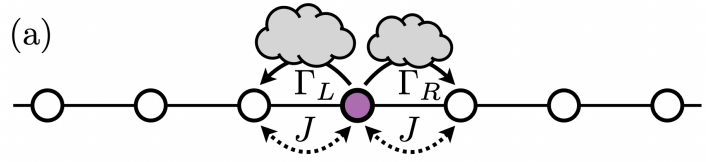

$$\hat{\mathcal{H}} = J \sum_{i=1} \left(\hat{c}_i^\dagger \hat{c}_{i+1} + \hat{c}_{i+1}^\dagger \hat{c}_i \right)$$

where i labels the lattice sites and J is the coherent symmetric hopping rate

Dissipative hopping with $\hat{L}_{i,L} = \sqrt{\Gamma_L}\, \hat{c}_i^\dagger \hat{c}_{i+1}$ and $\hat{L}_{i,R} = \sqrt{\Gamma_R}\, \hat{c}_{i+1}^\dagger \hat{c}_i$

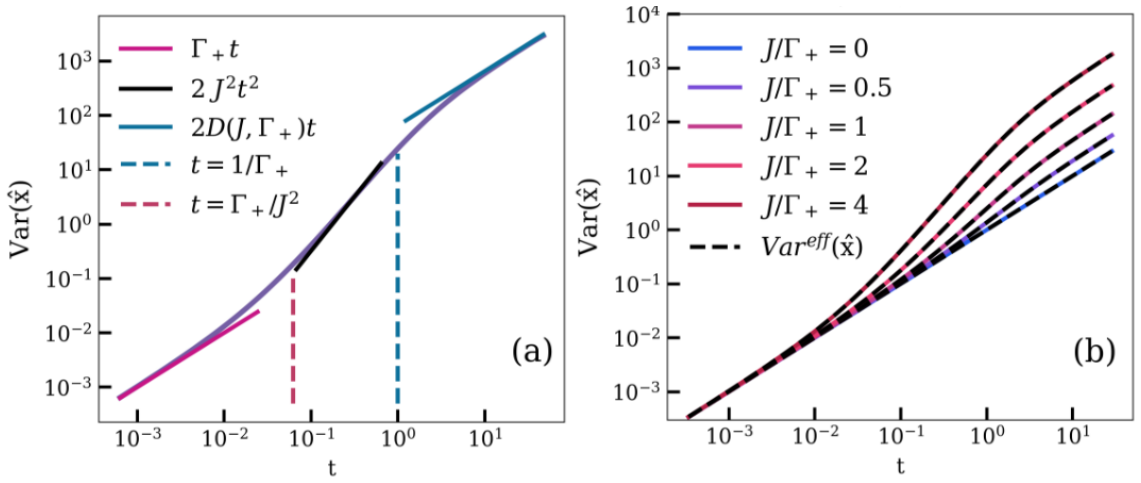

$$2\Gamma_+ = \Gamma_L + \Gamma_R$$

Crossover times

$$\tau^* = \Gamma_+ / J^2$$

$$t_R = 1/\Gamma_+$$

Effective Péclet

$$\mathrm{Pe} = J/\Gamma_+$$

Diffusive Ballistic Diffusive $D = \frac{\Gamma_+}{2}\left(1 + \frac{4J^2}{\Gamma_+^2}\right)$

Environment-assisted hopping

on an open one dimensional lattice with length L

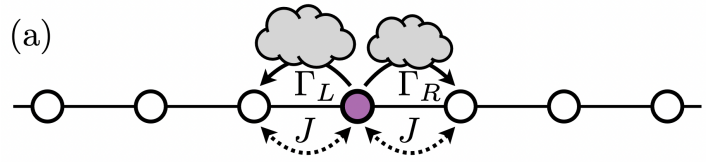

$$\hat{\mathcal{H}} = J \sum_{i=1} \left(\hat{c}_i^\dagger \hat{c}_{i+1} + \hat{c}_{i+1}^\dagger \hat{c}_i \right)$$

where i labels the lattice sites and J is the coherent symmetric hopping rate

Dissipative hopping with $\hat{L}_{i,L} = \sqrt{\Gamma_L}\, \hat{c}_i^\dagger \hat{c}_{i+1}$ and $\hat{L}_{i,R} = \sqrt{\Gamma_R}\, \hat{c}_{i+1}^\dagger \hat{c}_i$

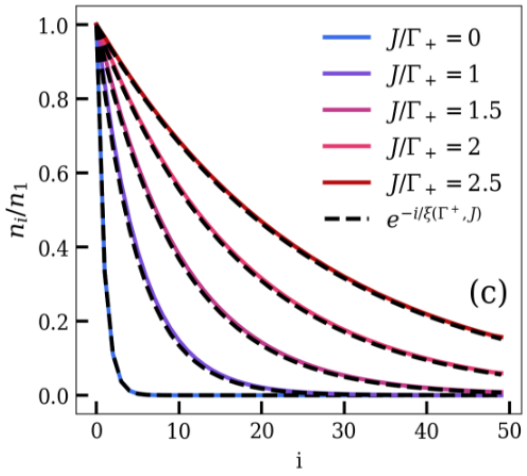

Asymptotic density profile

$$\Gamma_- = \Gamma_L - \Gamma_R > 0$$

$$n_i/n_1 = e^{-(i-1)/\xi}$$

$$\xi \sim \frac{D}{\Gamma_-} = \frac{\text{Diffusion}}{\text{Drift}}$$

as in **Tailleur & Cates 08, Razin 20**

for classical active particles

Lindblad skin effect

Quantum ABP

Additional - internal - two-level variable

The internal spin flips couple to left-right motion on the continuous line

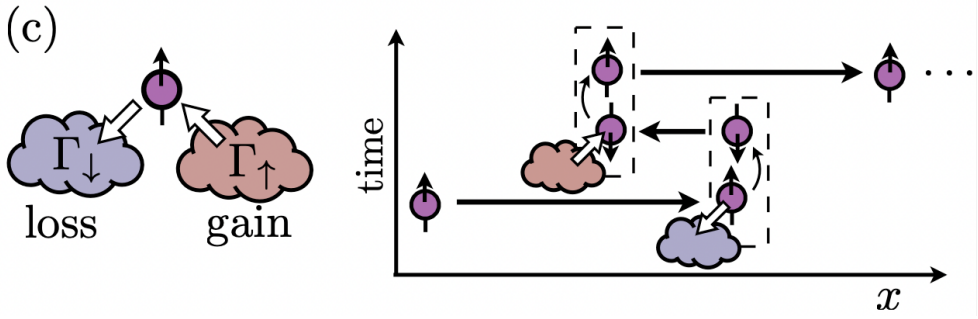

$$\hat{\mathcal{H}} = \frac{\hat{p}^2}{2m} + \lambda\,\hat{p}\hat{\sigma}_z$$

with $\hat{L}_\uparrow = \sqrt{\Gamma_\uparrow}\,\hat{\sigma}_+$ $\hat{L}_\downarrow = \sqrt{\Gamma_\downarrow}\,\hat{\sigma}_-$ $\hat{L}_d = \sqrt{\Gamma_d}\,\hat{p}$

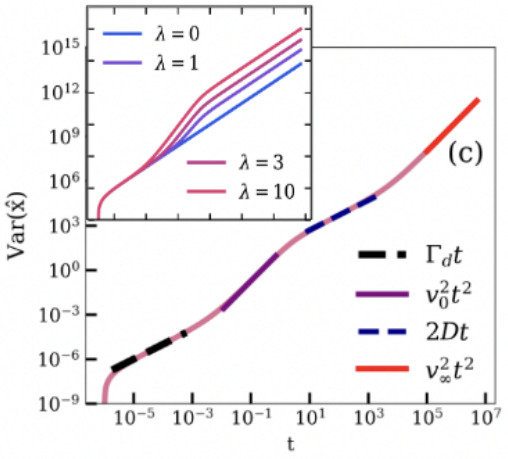

$$2\hat{\sigma}_\pm = \hat{\sigma}_x \pm \mathrm{i}\hat{\sigma}_y$$

Translation & internal d.o.f. feel different baths

$$D = \frac{\Gamma_d}{2}\left(1 + \frac{2\lambda^2}{\Gamma_d(\Gamma_\uparrow + \Gamma_\downarrow)}\right)$$

last ballistic regime

Quantum Active Particles

similar to Ornstein-Uhlenbeck

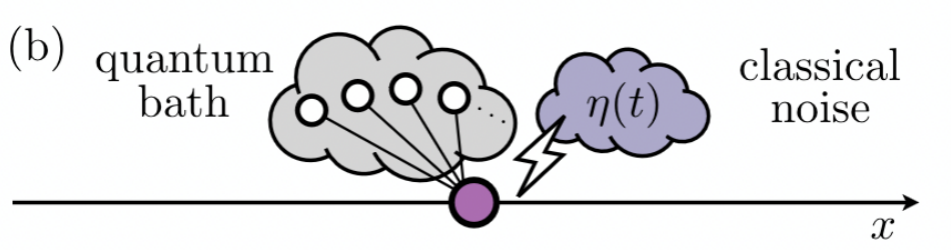

$$\hat{\mathcal{H}}_{\rm qAOUP} = \frac{\hat{p}^2}{2m} + \hat{\mathcal{H}}_{\rm bath}(\hat{x}) + g\hat{x}\eta(t)$$

Ohmic quantum dissipation

$$\hat{\mathcal{H}}_{\rm bath}(\hat{x}) = \sum_\alpha \left(\frac{\hat{p}_\alpha^2}{2m_\alpha} + \frac{m_\alpha \omega_\alpha^2}{2} \hat{x}_\alpha^2 \right) + \hat{x} \sum_\alpha g_\alpha \hat{x}_\alpha$$

spectrum $J(\omega) = \sum_\alpha \frac{g_\alpha^2}{m_\alpha \omega_\alpha} \delta(\omega - \omega_\alpha) = 4\gamma\omega \exp(-\omega/\omega_c)$

The classical noise $\eta(t)$ has zero mean and $\langle \eta(t)\eta(t') \rangle = \frac{D_\eta}{\tau} e^{-|t-t'|/\tau}$

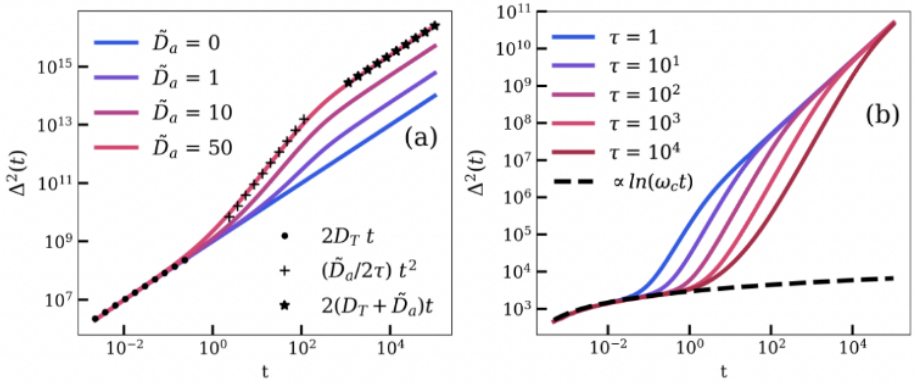

Schwinger-Keldysh - Closed time path integral

Diffusive – Ballistic – Diffusive

$$\tilde{D}_a = D_\eta / 4\gamma^2$$

$$D = D_T + \tilde{D}_a$$

Quantum Active Particles

Realizations

(a) **Environment assisted hopping on a lattice**

- Laser assisted hopping

(b) **Quantum Ornstein - Uhlenbeck particles**

- Superconducting circuits & Josephson junctions
- Impurities in cold atoms
- Optomechanics

(quantum Brownian motion) supplemented by a colored non-Markovian classical noise

(c) **Quantum Active Brownian Particles**

- Spin-to-momentum coupling can be engineered in atomic physics

Plan

1. Classical Active Matter
   - Real and artificial systems
   - Models
   - Phenomenology
2. Quantum Active Matter
   - Models
   - Phenomenology
   - Realizations ?
3. **Perspectives**